universität wien

# MASTERARBEIT / MASTER'S THESIS

Titel der Masterarbeit / Title of the Master's Thesis

**„The morphology of the feeding apparatus in *Aphanius mento*."**


verfasst von / submitted by

Christina Kaurin BSc


angestrebter akademischer Grad / in partial fulfilment of the requirements for the degree of

Master of Science (MSc)

Wien, 2019 / Vienna 2019

| | |
|---|---|
| Studienkennzahl lt. Studienblatt / degree programme code as it appears on the student record sheet: | A >066 831< |
| Studienrichtung lt. Studienblatt / degree programme as it appears on the student record sheet: | Masterstudium Zoologie UG2002 |
| Betreut von / Supervisor: | Dr. Christian J. Beisser |
| Mitbetreut von / Co-Supervisor: | |

# Table of contents

# 1 Abstract

*Aphanius* is a genus of pupfishes belonging to the family Cyprinodontidae of ray-finned fish. Unlike other members of this family, which are from America, *Aphanius* species are native to northern Africa, southwestern Asia (as far east as India) and southern Europe. They are present from the Mediterranean coasts of the Iberian Peninsula to the Red Sea and the Persian Gulf basins.

*Aphanius* primary occurs in freshwater habitats or coastal marine environments, characterized by warm water and mesosaline to hypersaline conditions.

Most *Aphanius* species are threatened because of drought, habitat degradation and loss, as well as water pollution, and the introduction of invasive species, like *Gambusia*.

*Aphanius* species feed on insect larvae, crustaceans and algae. Therefor they use suction feeding as a mechanism of prey capture. This led to some adaptations like a special mechanism of jaw protrusion.

The objective of this theses is to reconstruct the morphology of the feeding apparatus in *Aphanius mento* (provided by the Vienna zoo), for comparison with related groups, as well as to prepare a foundation for further kinematic studies.

To investigate the skeletal elements (skull, jaw elements, hyoid apparatus) as well as the appertaining musculature, microCT scans in combination with the software Amira were used. Furthermore, the specimens' skeleton was prepared via clearing and staining, a process that renders the flesh invisible, the bone red, and the cartilage blue.

Due to the structure of the skeletal elements in combination with the associated musculature in *A. mento* it is reasonable to conclude that within this species the maxilla is pulled forward as the lower jaw is depressed, resulting in the Type B mechanism of jaw protrusion, also known as "twisting maxilla model". A similar type of jaw arrangement and therefore a similar mechanism of jaw protrusion is present in *Poecilia sphenops*, *Fundulus* sp. and *Mugil* sp..

Furthermore, *A. mento*'s mouth region shows a beaklike appearance, well-suited for the mechanism of suction feeding, as well as picking prey from the surface of the water or the ground. The same beaklike appearance can be seen in *Gambusia affinis* and *Kryptolebias marmoratus*.

This study is also the first detailed description of *A. mentos* morphology and therefore has brought new insights concerning the anatomy of its feeding apparatus.

# 2 Zusammenfassung

*Aphanius* repräsentiert eine Gattung innerhalb der Ordnung der Zahnkärpflinge (Cyprinodontiformes) und der Familie der Cyprinodontidae. Während ein Großteil der Cyprinodontidae in Amerika beheimatet ist, erstreckt sich das Verbreitungsgebiet der verschiedenen *Aphanius* Arten vom südlichen Europa, über Afrika bis hin nach Südwest Asien.

*Aphanius* kommt in erster Linie im Süßwasser, sowie in marinen Küstengebieten vor, welche sich durch mesosaline bis hypersaline Bedingungen auszeichnen.

Die meisten *Aphanius* Arten sind aufgrund von Dürre, Habitats-Rückgang oder -Verlust, sowie Wasserverschmutzung und das Ansiedeln invasiver Arten (z.B. *Gambusia*) bedroht.

*Aphanius* ernähren sich in erster Linie von Insektenlarven, Krustentieren und Algen, wodurch diese Gattung einige Anpassungen im Hinblick auf die Nahrungsaufnahme und die damit verbundene „jaw protrusion" aufweist.

Im Zuge dieser Masterarbeit wurde die Schädelmorphologie von *Aphanius mento* untersucht, um diese anschließend mit anderen Gruppen zu vergleichen. Ziel war es auch, eine Grundlage für weitere kinematische Arbeiten zu schaffen.

Von den vom Zoo Schönbrunn zur Verfügung gestellten Tieren wurden microCT Scans angefertigt, um anschließend die Knochenelemente sowie die damit verbundene Muskulatur im Programm Amira zu rekonstruieren. Um die Knorpelelemente zu visualisieren, wurde die Methode des „clearing and staining" verwendet, wodurch die Knochen rot und die Knorpel blau gefärbt wurden.

Aufgrund der Schädelmorphologie wird davon ausgegangen, dass *A. mento* den Typ B Mechanismus, auch bekannt als „twisting maxilla model", der „jaw protrusion" aufweist. Dabei wird die Maxilla nach vorne gezogen, während der Unterkiefer nach unten bewegt wird. *Poecilia sphenops, Fundulus sp. and Mugil sp.* weisen einen ähnlichen Kieferaufbau und dementsprechend auch eine ähnliche „jaw protrusion" auf. Die Mundregion von *A. mento* weist ein „schnabelartiges" Erscheinungsbild auf. Dieses ist sowohl für den Mechanismus des Saugschnappens, als auch für das „Aufpicken" von Nahrung vom Grund und von der Wasseroberfläche gut geeignet. Das gleiche „schnabelartige" Erscheinungsbild kann man auch bei *Gambusia affinis* und *Kryptolebias marmoratus* erkennen.

Im Zuge dieser Arbeit wurde die Schädelmorphologie von *A. mento* das erste Mal sehr detailliert dargestellt und beschrieben und liefert somit neue Erkenntnisse bezüglich der Anatomie dieser Tiere.

# 3 Introduction

Taking a look at the evolutionary history of feeding mechanisms and biomechanics in fish, there are a lot of morphological changes, including the structure and function of kinetic vertebrate skull. Regarding morphology and kinematics, the fish skull is very complex, leading to diverse feeding mechanisms (Westneat, 2006). The dietary preferences within different groups of fishes (piscivores, herbivores, planktivores, detritivores, molluscivores etc.) determine the feeding mechanism of each species. Mechanisms using water flow are for example inertial suction, where the prey is drawn into the mouth while the animal remains stationary, and compensatory suction, where the prey is kept in place, while the animal lunges at it (Gilles et al., 1994; van Damme and Aerts, 1997). This trophic strategies include biting tough, encrusted algae (Bellwood and Choat, 1990), sucking miniscule crustaceans from the water column (Bergert and Wainwright, 1997), scraping epiphytic algae from the substrate (Schaefer and Lauder, 1986), suspension feeding on zooplankton and phytoplankton from the water column (Goodrich et al., 2000), ambush attacks on mobile prey (Lauder and Liem, 1981), rotational feeding to tear chunks from larger prey (Helfman and Clark, 1986), and feeding on highly elusive prey (Sanford and Wainwright, 2002; Hernandez et al., 2008).

## 3.1 Mechanism of suction feeding

The high density and viscosity of the water complicates the interaction between fish and their food particles. Thus, to take up their food, fish using suction feeding have to create a water flow through their buccopharyngeal cavity (Gilles et al., 1994). This can be achieved by ram feeding, where both the mouth and the opercula are widely opened during swimming, or by means of active suction (inertial suction) (Lauder 1985; Gilles et al., 1994).

Inertial suction feeding is the most common mechanism of prey capture in fish and other aquatic vertebrates (e.g., Alexander 1969; Liem 1979; Lauder 1980b, 1980c, 1985; Lauder and Shaffer 1985; Lauder and Reilly, 1994; Lauder and Prendergast 1992; Svaänback et al., 2002), and probably was employed by the earliest gnathostomes (Lauder, 1985; Moss, 1977; Gibb and Ferry-Graham, 2005). It presupposes a rapid expansion of the buccal and opercular cavities, thus drawing the prey into the mouth along with the surrounding water (Lauder, 1980a; Lauder, 1985; Aerts et al., 1991; Ferry-Graham and Lauder, 2001). The produced suction force can vary among species depending on the size and elusiveness of the prey. Also, while soft prey may be swallowed as soon as it is captured, hard prey, such as shelled invertebrates, often require additional physical processing. To enable this feeding mechanism, the fish skull contains about

60 interconnected skeletal elements that can be moved in a coordinated way (Aerts, 1991). To allow such movement, an equal amount of muscles have to take action. In bony fish, the mechanism of suction feeding can be structured in four phases: (I) 'preparatory' phase, (II) 'expansive' phase, (III) 'compressive' phase, and (IV) 'recovery' phase (Muller and Osse 1984; Lauder, 1985; Lauder and Reilly, 1994; Gibb and Ferry-Graham, 2005; Helfman et al., 2009).

During the preparatory phase, the buccal cavity is first compressed, followed by a rapid expansion during the ‘expansive’ phase. In terms of suction feeding, this phase is of utmost importance. The overall change in buccal volume, as well as the velocity with which it occurs affect the generation of flow into the mouth (Lauder, 1980a; van Leeuwen and Muller, 1984; Muller, 1987; Gibb and Ferry-Graham, 2005). Furthermore, an anterior-to-posterior wave of expansion is created by components of the head and jaws (Lauder, 1985; Muller and Osse, 1984; Gibb and Ferry-Graham, 2005). Therefore, any given cranial element reaches the limit of its excursion slightly before the element immediately posterior to it (Gibb and Ferry-Graham, 2005). Thereby, in the cranium of Osteichthyes, first the lower jaw reaches its maximum depression, followed by the neurocranium achieving its maximum rotation and the opercular region reaching its maximum expansion. After the expansive phase, the water gets expelled through the opercular openings or the mouth of the fish. Meanwhile, the food is retained in the oral jaws or the buccal cavity. This compressive phase is, in comparison to the previous phase, significantly slower. During the recovery phase the elements finally return to their relaxed prefeeding position. These four phases may be repeated cyclically to produce the flow of water necessary to transport the food into the esophagus (e.g., Gillis and Lauder, 1995).

## 3.2 Premaxillary movements in cyprinodontiform fish

Another important part allowing the ingestion of food is the jaw protrusion. It comes with several advantages during prey capture, for example an increase in prey capture velocity and a shortening of the predator-prey distance (Norton and Brainerd, 1993), by allowing the fish to protrude a small element rapidly towards the prey. Furthermore, it increases the water velocity - and therefore suction force - during feeding (Schaeffer and Rosen, 1961; Motta, 1984; Norton and Brainerd, 1993), as well as enabling a fish to close its mouth rapidly by decreasing the distance between upper and lower jaws (Alexander, 1967a).

Jaw protrusion is characteristic for many acanthopterygian teleosts (Greenwood et al., 1966). It involves the anterior, anteriodorsal or anterioventral movement of the upper jaw and the pivoting of the lower jaw or mandible around a ball and socket articulation with the suspensorium such that the entire mouth is moved anteriorly (Greenwood et al., 1966, Motta, 1984).

To consume the prey, teleostei have evolved 4 different ways of premaxillary protrusion (Motta, 1984).

In Type A, also called "mandible depression model" of jaw protrusion, the premaxilla is pulled or pushed into the protruded state due to depression of the mandible (Eaton, 1935; Alexander, 1967a, b; Lauder, 1982; Motta, 1984). The created force may be transferred to the upper jaw via bones, ligaments or tendons. The twisting of the maxilla around its longitudinal axis may occur passively in comparison to the Type B or "twisting maxilla model" (Motta, 1984). In this type, the twisting of the maxilla round its longitudinal axis is used to drive or pull the premaxilla into the protruded position (Motta, 1984). Either depression of the mandible or contraction of the A1 division of the adductor mandibulae musculature initiates the twisting mechanism (Alexander, 1967b; Liem, 1980a; Motta, 1984). In Type C or "decoupled model" of jaw protrusion, the neurocranium is lifted independently from the premaxilla resulting in protrusion of the latter. In Type D or "suspensorial abduction model", the latter two mechanisms are augmented by abducting the suspensorium to produce tension in the palatopalatine ligament, pushing the ascending process of the premaxilla such that protrusion of the premaxilla occurs (Liem, 1980a; Motta, 1984).

Cypriniformes and Percomorpha represent two of the largest and most successful groups of teleost fishes (Ferry-Graham et al., 2008). In both orders, a mobile bony element formed by the paired premaxilla bones projects towards the prey during feeding (Lauder and Liem, 1983). In perspective of the general lineage of Cypriniformes as well as the general perciform lineage, the movement of the upper jaw during feeding consists of the premaxilla rotating dorsally and concurrently projecting ventrally. This anterior movement of the paired descending processes serves to occlude the sides of the v-shaped mouth opening to prevent the prey from escaping through the sides of the mouth (Motta, 1984; Ferry-Graham et al., 2008). Simultaneously, the anterior movement of the descending processes helps to form a tubular mouth opening that is associated with increased suction production during prey capture (Norton and Brainerd, 1993; Wainwright et al., 2001; Wainwright and Day, 2007; Ferry-Graham et al., 2008).

However, Cyprinodontiformes, including the genus *Aphanius*, are a large and successful group of teleosts that demonstrate a notably different upper jaw protrusion mechanism (Ferry-Graham et al., 2008). In Cyprinodontiformes, the descending processes of the maxilla are bound by taut ligaments to the mandible. Therefore, the descending processes cannot swing anteriorly during the mouth opening, resulting in not occluding the sides of the opened mouth. The dorsal elements of the premaxilla protrude in a ventral direction, creating a beaklike appearance during the feeding mechanism (Ferry-Graham et al, 2008).

During the protrusion, a lip membrane is pulled taut and serves in some taxa to partially occlude the sides of the open mouth.
In conclusion, the mechanism of jaw protrusion within the Cyprinodontiformes differs in both underlying morphology and mechanics of movement from other orders.

Besides the skeletal elements, the musculature plays an important part in capturing the prey. To give an example, the m. adductor mandibulae complex is highly adapted to different feeding strategies among vertebrate clades leading to a large amount of diversification (Gosline, 1986; Diogo, 2008; Diogo and Abdala, 2010; Datovo and Vari, 2013; Werneburg, 2015).

## 3.3 Kinematic

In addition to morphological adaptions, kinematic patterns of the oral jaw (gape), hyoid (depression) and suspensorium (abduction) are important in triggering suction production. The cranial elements involved in these patterns - jaw, neurocranium, hyoid and opercular bones - operate as an integrated structural complex (Sanford and Wainwright, 2002; Gibb and Ferry-Graham, 2005). This implies that an individual fish may change the amount of suction produced by manipulating the timing or maximal displacement of all four cranial elements at once (Gibb and Ferry-Graham, 2005). If individuals of a species specialize on more challenging prey, they modify their mechanism of suction feeding by modifying their prey-capture kinematics or by changing their feeding morphology (Gibb and Ferry-Graham, 2005). For example, fish with smaller mouths and deeper bodies continue to produce greater suction pressure during feeding compared to fish with larger mouths and shallower bodies (Carroll et al., 2004; Gibb and Ferry-Graham, 2005). This enables them to capture more elusive prey. Clearly, changes in morphology are highly correlated with changes in suction pressure, but it is also important to note that changes in feeding kinematics are another key element in enhancing the suction produced.

## *3.4 Aphanius mento*

Killifish (Cyprinodontiforms), including the genus *Aphanius*, are a large group of secondary freshwater fish and have proven to be particularly interesting for evolutionary studies (see review in Parker and Kornfield, 1995; Teimori et al., 2014). They are widely distributed along the late-period Tethys Sea coast lines (Güçlü and Küçük, 2008; Güçlü, 2012). However, the current distribution area of *Aphanius* has also been influenced by glacial and interglacial period differences in the Mediterranean Sea level (Wildekamp et al., 1999; Güçlü and Küçük, 2008).

The genus *Aphanius* is composed of 30 species comprising two major clades that most likely developed near coastal areas during the closing of the Tethys Sea (Hrbek and Meyer, 2003). The current distribution area of *Aphanius mento* ranges from the Arabian Peninsula, Syria and Lebanon to the coastal rivers in Israel and Western Jordan (Güçlü and Küçük, 2008), where it inhabits fresh to lightly brackish water in springs, creeks, rivers and small lakes near the banks. It is predominantly found in marginal zones amongst or close to vegetation where males establish their territories (Wildekamp, 1993; Wildekamp et al., 1999). Like most cyprinodontiforms, species of *Aphanius* tolerate a wide range of temperatures and salinities (Teimori et al., 2014). This ecological tolerance, in combination with their small size and their feeding spectrum (insect larvae, crustaceans, and algae) permits *Aphanius* populations to persist in restricted and extreme habitats (e.g., Echelle and Dowling, 1992; Wildekamp, 1993; Teimori et al., 2014).
An example of a typical habitat can be found in Antalya province, Turkey. The Kirkgöz spring, characterized by its relatively high levels of salts, containing chlorine, magnesium and calkin, originates from karstic limestones and flows for around 30km before emptying into the Gulf of Antalya (Güçlü and Küçük, 2008).
The genus *Aphanius* is well known for its expulsion due to invasive species of the genus *Gambusia*. Latter were introduced to the environment by humans to control the mosquito population because they prey on mosquito larvae. The introduction of *Gambusia holbrooki* caused a decrease in the number of frogs (Webb and Joss, 1997; Mordenti et al., 2012), markedly reduced the population density of invertebrate predators of mosquitoes (El Safi et al., 1985; Mordenti et al., 2012), whereby affected *Aphanius* populations (Caiola and Sostoa, 2005; Mordenti et al., 2012). Several studies have investigated *Aphanius* as a potential biological control agent for mosquito larvae (Al-Akel and Suliman, 2011; Haq and Srivastava, 2013).

The focus of this study lies on the morphology of the feeding apparatus (skull, hyoid apparatus and associated musculature) in *Aphanius mento* with the aim to describe the anatomy of *Aphanius mento* in detail and thereby prepare a foundation for further anatomical and kinematic studies.

# 4 Materials and Methods

To investigate the skeletal elements (skull, jaw elements, hyoid apparatus) and the appertaining musculature of *Aphanius mento*, microcomputed tomography scans (μCT) were used. The individual fish were provided by the Vienna Zoo (Vienna, Austria). One individual was scanned using microcomputed tomography scans by Stephan Handschuh at the Imaging Unit of the VetCore Facility for Research at the University of Veterinary Medicine Vienna (Austria). The specimen was scanned with the Zeiss Xradia MicroXCT-400 (Carl Zeiss X-ray Microscopy, Pleasanton, CA, USA).

For μCT, the specimen was anesthetized with a lethal dose of Tricaine (MS 222), fixed in 4% formaldehyde solution for 1year, and stained for six days, using 1% $I_2$ in EtOH. Afterwards it was washed and mounted in 100% EtOH. To distinguish soft tissues (musculature) from hard tissue (skeletal elements) in a single sample, two different x-ray energy spectra (40kVp and 80kVp) were used and a dual energy scan of 40/80 kVp was performed (for details on the method, see Handschuh et al., 2017).
The x-ray source settings of the low energy scan were 40kVp and 200μA, while the higher energy scan was conducted with 80kVp and 100μA. Projection images were recorded using a 4x optical lens and an angular increment of 0,167° between projections and exposure times of 40s for 40 kVp and 20s for 80 kVp. Voxel size of both low and high energy scans were 6,77μm.

For the 3D reconstruction of the skull, the jaw elements, the hyoid apparatus and the appertaining musculature, Amira 6.3 and 6.4 (FEI, Oregon, USA) were used. Additionally, the Amira Volren Tool, which provides a volume rendering of either the skeletal elements or other body tissues, was applied to the μCT scan of *A. mento*.
To create the reconstructions, each skeletal element and muscle was selected on multiple slices using the segmentation editor, interpolated where possible, and assigned to a label. The segmented elements were then visualized using the Surface Generation Tool and optimized by iterated simplification and smoothing tools. The 3D reconstructions were displayed and snapshots were taken.

Due to technical reasons, the resolution of the scans can occasionally lead to limitations on the reconstructions. For example, thin tissues like tendons or thin skeletal elements are difficult to reconstruct. Also, the borders between different muscles as well as those between some skeletal elements are sometimes difficult to pinpoint. After using the simplification and smoothing tools,

a scalebar was added and snapshots of the finalised reconstructions were taken. Names of muscles and skeletal elements were added using Photoshop CC (Adobe Photoshop CC, Adobe Systems, Delaware USA).

In addition to the 3D reconstructions, one specimen's skeleton was prepared using clearing and staining. The formaldehyde fixated fish was rinsed in distilled water and then dehydrated in 50% EtOH for 24 hours. Afterwards, the specimen was transferred to 100% EtOH for 24 hours. Cartilage were stained in a solution consisting of 70ml 100%EtOH, 30 ml acetic acid, 20mg Alcian blue. After the staining process the fish was moved directly to a saturated sodium borate solution for about half a day. This step is called neutralisation and will prevent calcium loss during bleaching. The next step was to bleach the specimen by using 15 ml 3% hydrogen peroxide ($H_2O_2$) in 85 ml 1% potassium hydroxide (KOH) solution. Afterwards, the fish was put into a clearing solution of 35ml saturated sodium borate, 65ml distilled water and 1% trypsin. The specimen was kept in the clearing solution until about 60% clear. To stain the skeletal elements, KOH and the Alizarin Red stain were mixed together. After 1 day the fish was put in a destaining solution, where it stayed for 2 days. Therefor, 35 ml saturated sodium borate solution, 65 ml distilled $H_2O$ and trypsin powder were used.
For preservation 30% glycerine and 70% KOH were used. One week after the clearing and staining procedure, images of *A. mento* were taken using the stereomicroscope Nikon SMZ25 in combination with the camera Nikon DS-Ri2.
Finally, the visible structures were labelled, again using Photoshop CC (Adobe Photoshop CC, Adobe Systems, Delaware USA).

# 5 Results

The aim of this study was to image and analyse the skull, hyobranchial apparatus and muscles involved in the feeding process of *Aphanius mento*.

The head of a fish can be divided into six main regions: the cranium, the jaws, the cheeks, the hyoid arch, the opercula, and the branchial arch. On the posterior side of the head, a pectoral girdle separates the head region from the rest of the body.

"A Descriptive Synonymy of the Striated Muscles of the Teleostei" (Winterbottom, 1973) and "Morphology of a picky eater: A novel mechanism underlies premaxillary protrusion and retraction within cyprinodontiformes" (Hernandez et al., 2008), were used as guidelines for the nomenclature in this study.

## 5.1 Skeletal elements

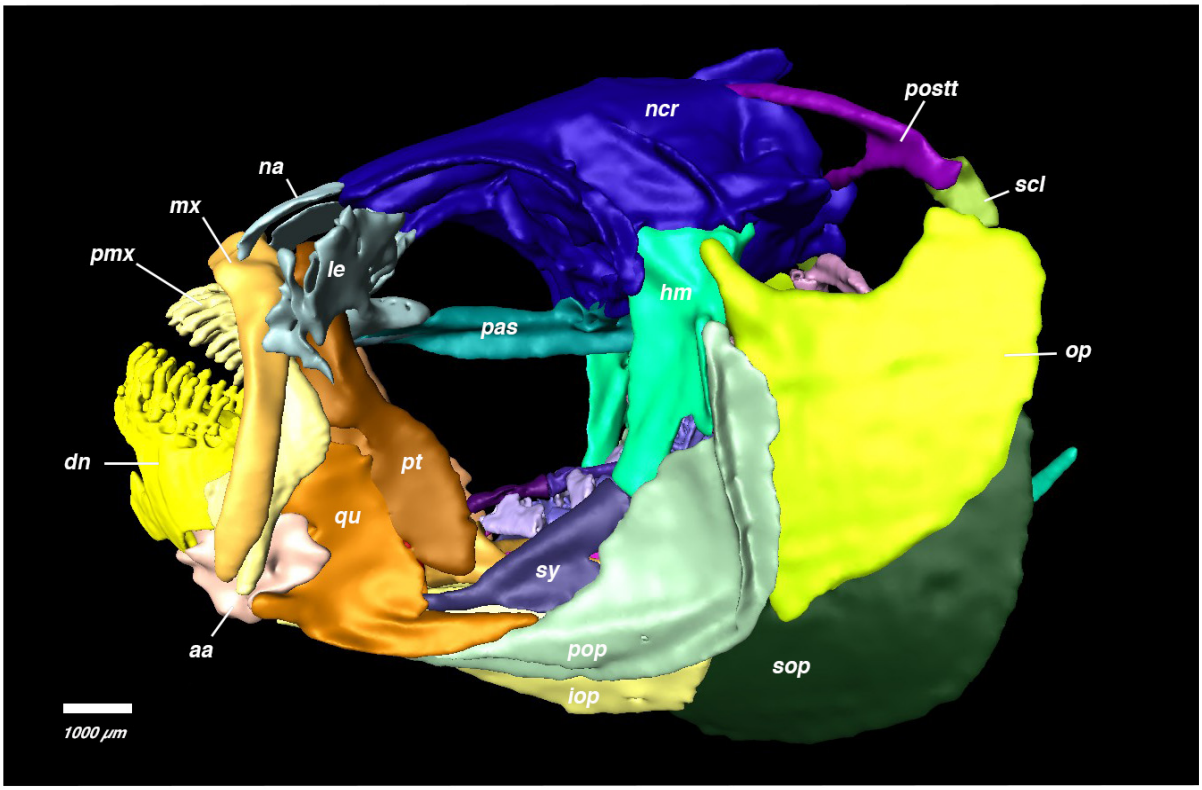


**Figure 1:** Lateral view of the reconstructed skull of *Aphanius mento*, without cartilage, ligaments or muscles. **aa** = angulo-articular, **dn** = dentary, **hm** = hyomandibular, **iop** = interopercular, **le** = lateral ethmoid, **mx** = maxilla, **na** = nasal, **ncr** = neurocranium, **op** = opercular, **pas** = parasphenoid, **pop** = preopercular, **pt** = pterygoid, **pmx** = premaxilla, **postt** = posttemporal, **qu** = quadrate, **scl** = supracleithrum, **sop** = subopercular, **sy** = symplectic.

The skull of *Aphanius mento* is composed of numerous important movable skeletal elements (Fig. 1). The skull of *A. mento* shows a short snout.

While most elements are ossified, a part of the ethmoid, the mesethmoid, is cartilaginous and has a dermal element fused to it (Fig. 2).

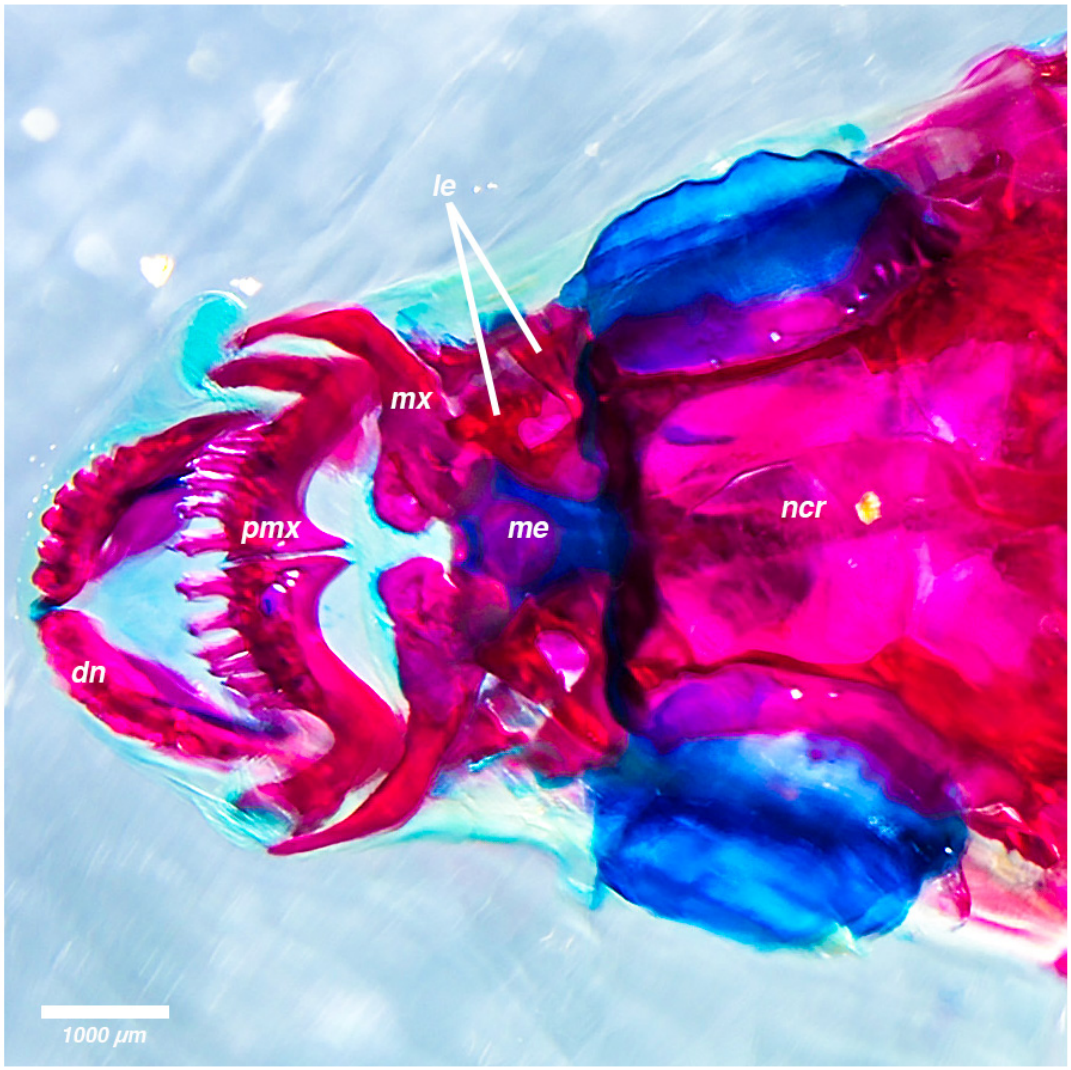


**Figure 2:** Dorsal view of *Aphanius mento* showing skeletal and cartilaginous elements of the head. Due to the method of clearing and staining, the bony elements are colored red and the cartilaginous elements are colored blue. **dn** = dental, **le** = lateral ethmoid, **me** = mesethmoid, **mx** = maxilla, **ncr** = neurocranium, **pmx** = premaxilla.

### 5.1.1 Neurocranium

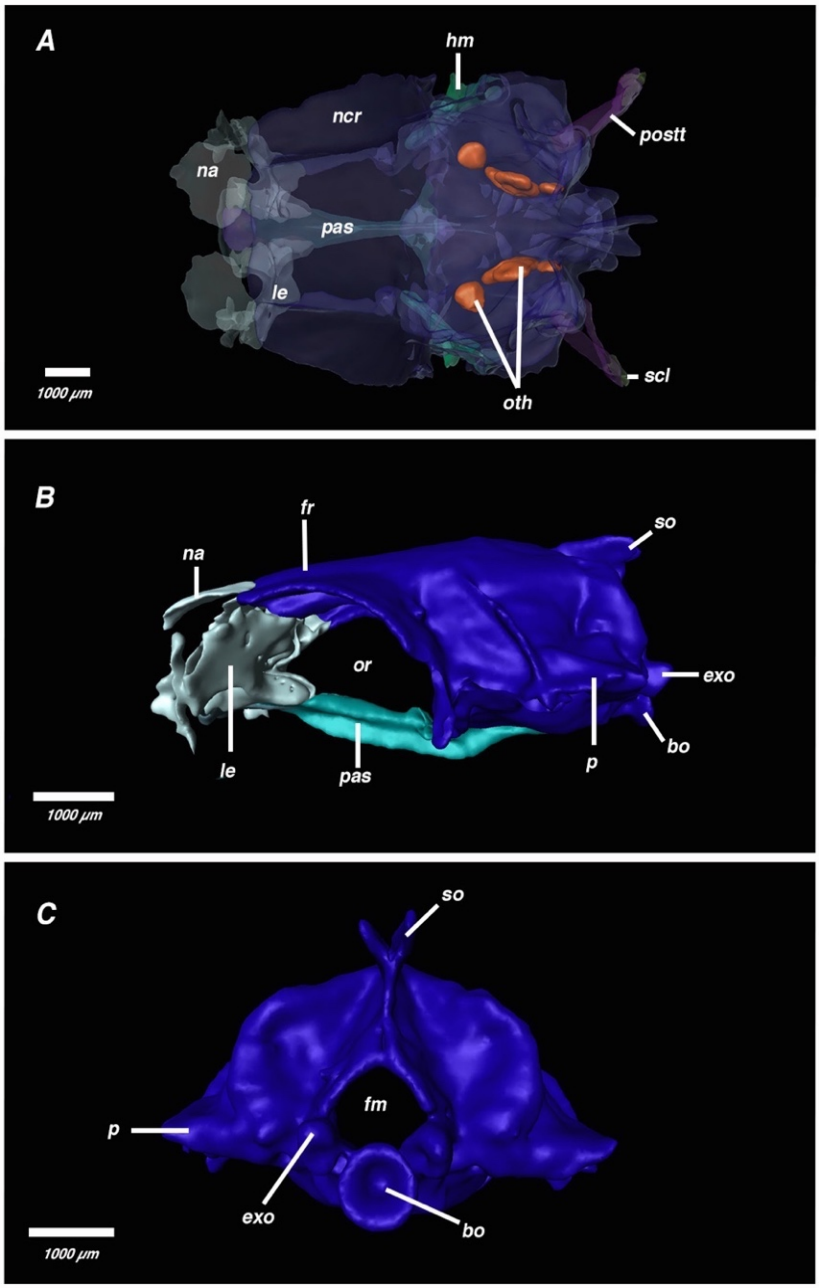


**Figure 3:** Dorsal **(A)**, lateral **(B)** and posterior **(C)** view of the reconstructed neurocranial region of *Aphanius mento*. In A the neurocranium is see-through, so that the otoliths can be seen. **bo** = basioccipital, **exo** = exoccipital, **fm** = foramen magnum, **fr** = frontal, **hm** = hyomandibular, **le** = lateral ethmoid, **na** = nasal, **ncr** = neurocranium, **oth** = otolith, **or** = orbit, **p** = pterotic, **pas** = parasphenoid, **postt** = posttemporal, **scl** = supracleithrum, **so** = supraoccipital.

The neurocranium consists of numerous bony elements (frontal, pterosphenoid, parietal, sphenotic, pterotic, supraoccipital crest, intercalar, exoccipital, basioccipital, prootic, parasphenoid, basisphenoid, vomer) that are merged. The frontal bone of the neurocranium surrounds the dorsal region of the orbit (Fig. 3B). Below the neurocranium is the parasphenoid, a bony element

that connects the vomer and ethmoid to the neurocranium (Fig. 3A/B). The supraoccipital is a median bone in the upper rear part of the skull, as can be seen in Fig. 3B/C.

The foramen magnum is the posteromedial aperture through the occiput into the cranial cavity, that is located above the basioccipital and between the exoccipital (Fig. 3C).

The three pairs of otoliths, shown in Fig. 3A, demonstrate the position of the inner ear. The largest one is called sagitta, and is positioned between the astericus and lapillus.

## 5.1.2 Splanchnocranium

### 5.1.2.1 Oral jaws

#### 5.1.2.1.1 Upper jaw

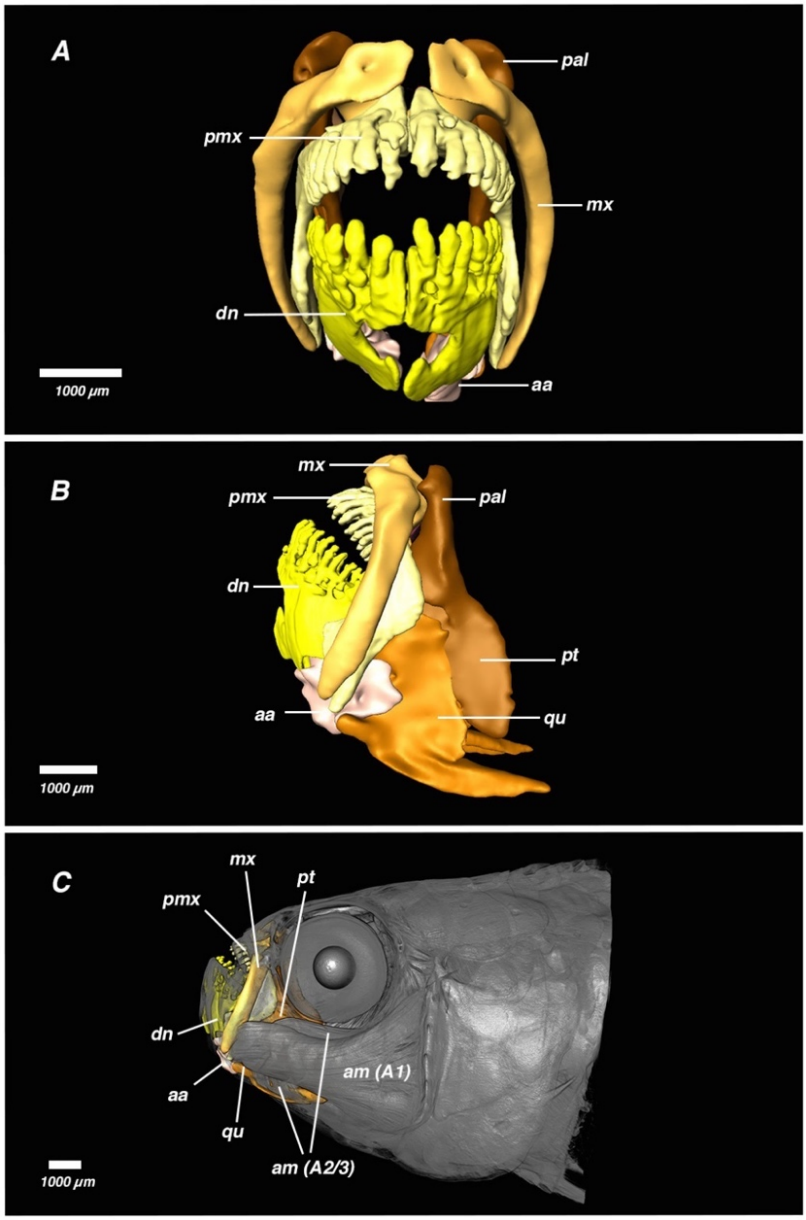


**Figure 4**: Anterior **(A)** and lateral **(B/C)** view of the oral region of *Aphanius mento*. **aa** = angulo-articular, **am** = adductor mandibulae, **dn** = dentary, **mx** = maxilla, **pmx** = premaxilla, **pal** = palatine, **pt** = pterygoid, **qu** = quadrate.

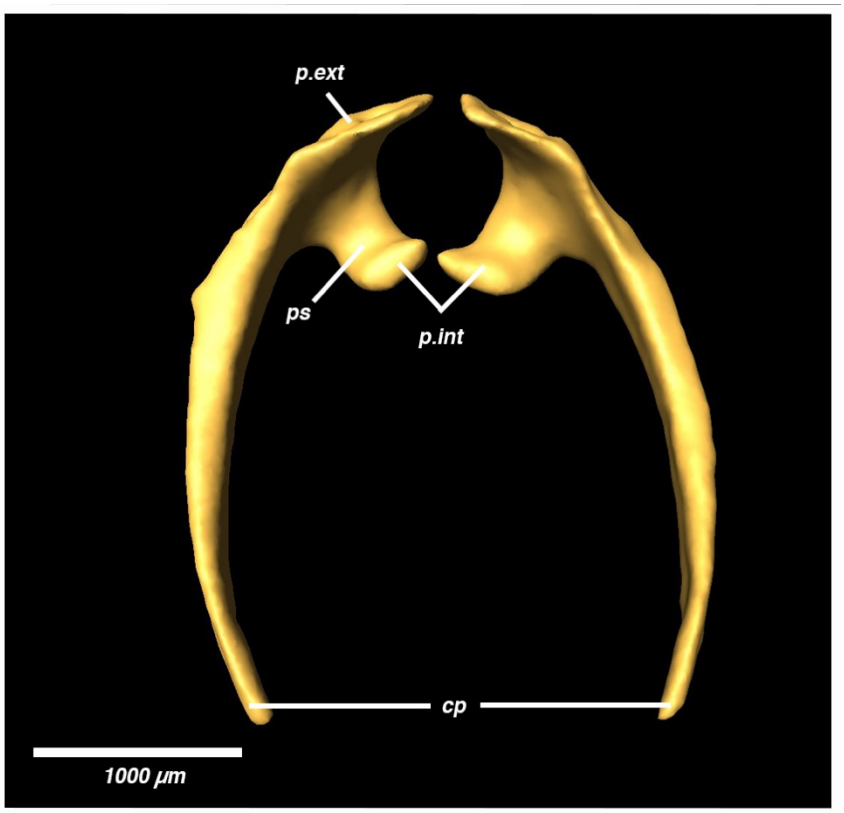


**Figure 5:** Anterior view of the 3D model of the maxilla of *Aphanius mento* in detail. **cp** = caudal process, **p.ext** = external process, **p.int** = internal process, **ps** = premaxillary sulcus.

The upper jaw consists of a paired maxilla and premaxilla (Fig. 4A). The toothless and elongated maxillae are located above the premaxillae (Fig. 4A-C, 5, 6). The ascending process of each maxilla is more complex, featuring an external and internal process, as well as a premaxillary sulcus (Fig. 5). The ventral ends of the descending arms, also known as maxillary or caudal process, are affixed firmly to the ventral end of the premaxilla.

The descending arms of the paired premaxillae have a recurved shape (Fig. 4A-C and Fig. 6). The ascending arms diverge from one another at their posterodistal ends. Between the dorsal ends of the ascending arms, connective tissue and rostral cartilages are present.

In Fig. 6 the shape of the premaxillary teeth can be seen. Each tooth shows three tips, with the one in the middle being the longest.

The pterygoid is a paired skeletal element connecting the palatine anteriorly to the quadrate posteriorly (Fig. 4B).

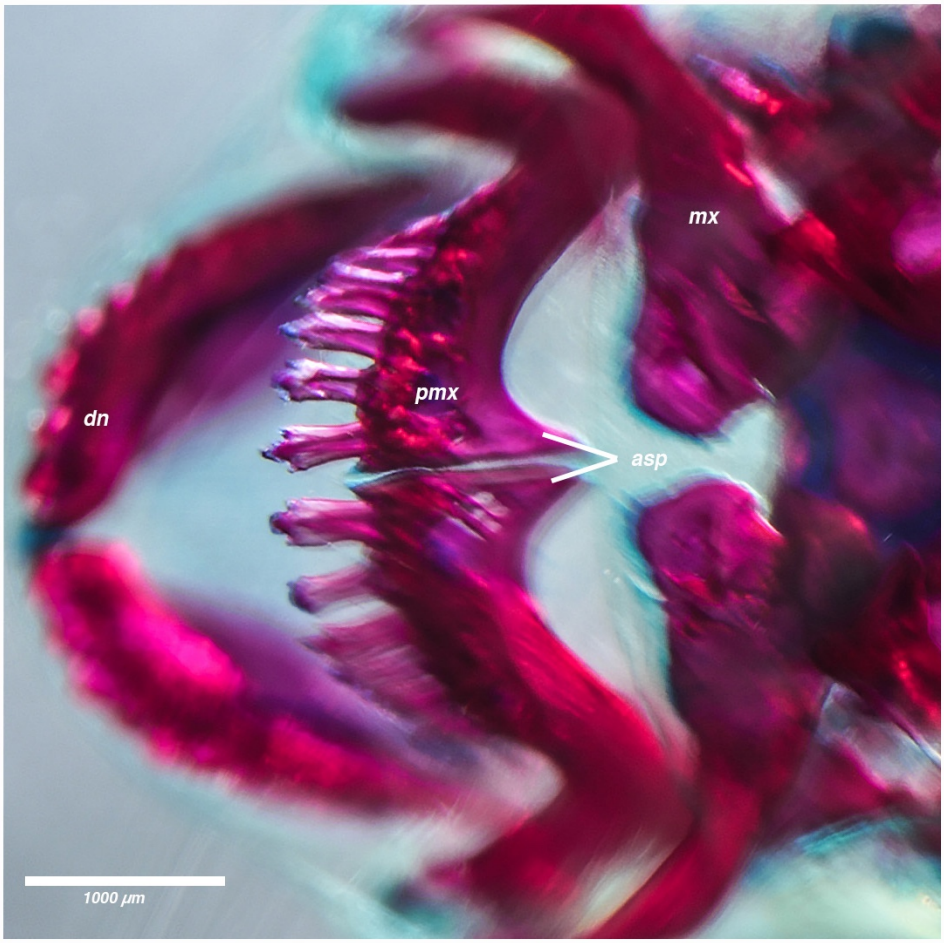


**Figure 6:** A closeup of the mouth region of *Aphanius mento*, showing the shape of the premaxillary teeth and the ascending processes of the premaxille. Due to the method of clearing and staining, the bony elements are colored red and the cartilaginous elements are colored blue. **asp** = ascending process, **dn** = dental, **mx** = maxilla, **pmx** = premaxilla.

#### 5.1.2.1.2 Lower jaw

The lower jaw shows a dentary bone and an angulo-articular (Fig. 4A-C, 7A/B). The pair of dentaries carry teeth and form the anterior part of the lower jaw. They hold/contain a peripheral row of tricuspid teeth similar to the premaxillary. The dentaries show ventral and dorsal processes where they articulate with the angulo-articular.

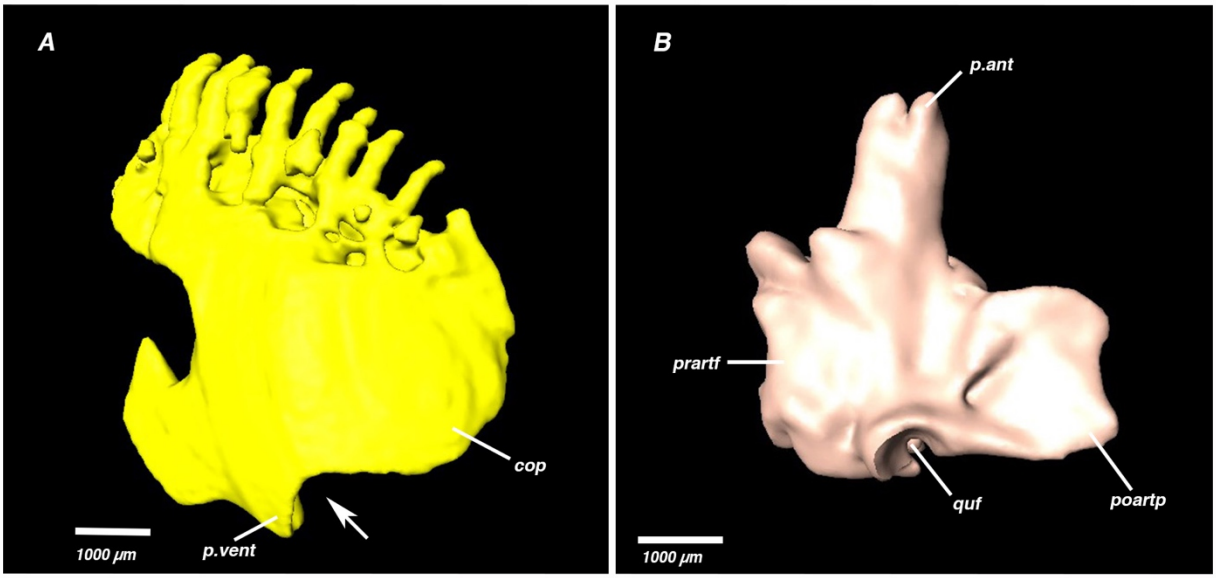


**Figure 7:** Lateral view of the 3D model of the dentary **(A)**, and the angulo-articular **(B)** in detail. The arrow points at the "V" shaped region of the dentary, where the anterior process of the angulo-articular inserts. **cop** = coronoid process, **p.ant** = anterior process, **poartp** = postarticular process, **prartf** = prearticular fossa, **p.vent** = ventral process, **quf** = quadrate facet.

The paired angulo-articular form the posterior part on either side of the lower jaw (Fig. 4A). This is also known as the 'angular complex' which consists of the fused angular, articular, and retroarticular. The anterior part of these bones articulates with the dentary via an anterior process, while the posterior part is connected to the suspensorium. The anterior process of the angulo-articular is quite long and inserts into the ''V'' which is formed by the two processes of the dentary (Fig. 7A/B).

The angular complex is triangular with a quadrate facet (Fig. 7B), which fits between the lateral and mesial condyles of the quadrate (Fig. 9). The Meckel's cartilage covers a large part of the articular (Fig. 8).

### 5.1.2.2 Suspensorium

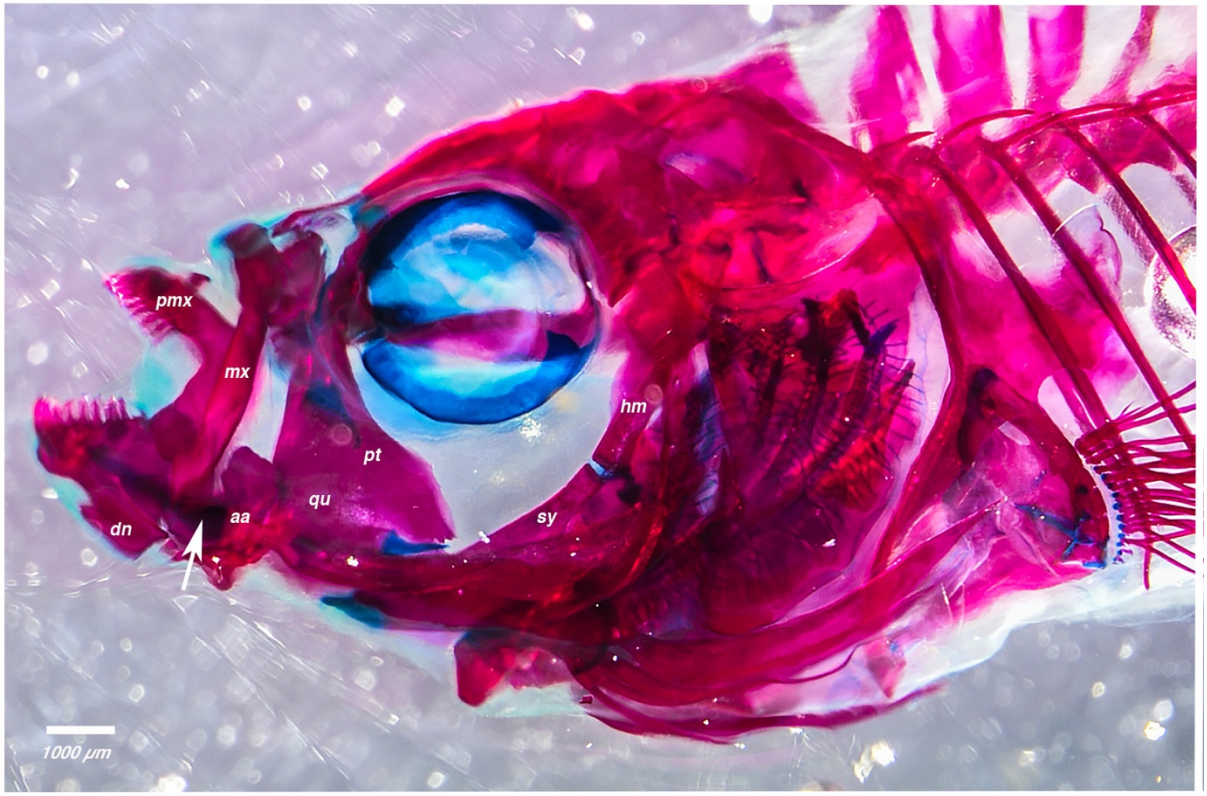


**Figure 8:** Lateral view of *Aphanius mento*. Due to the method of clearing and staining the bony elements are colored red and all the cartilages are stained blue. The arrow points at the Meckel's cartilage. **aa** = angulo-articular, **dn** = dental, **hm** = hyomandibular, **mx** = maxilla, **pmx** = premaxilla, **pt** = pterygoid, **qu** = quadrate, **sy** = symplectic.

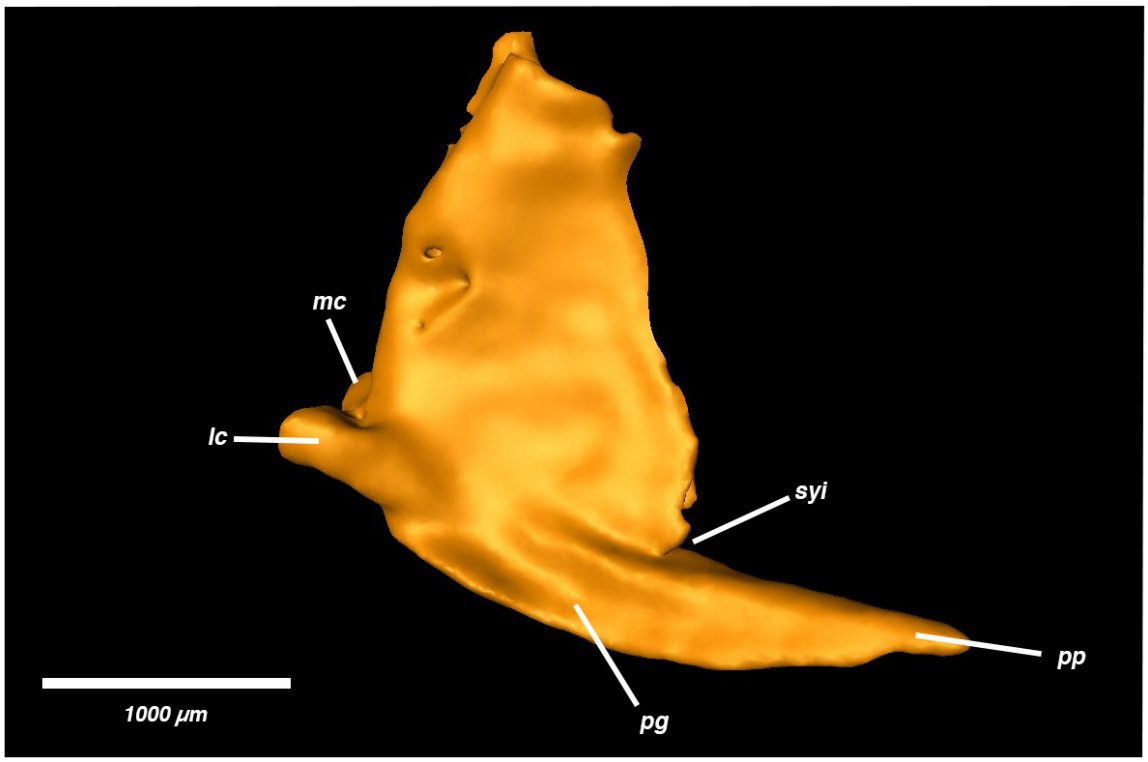


**Figure 9:** Lateral view of the 3D model of the quadrate *of Aphanius mento* in detail. **lc** = lateral condyle, **mc** = mesial condyle, **pg** = preopercular groove, **pp** = preopercular process, **syi** = symplectic incisure.

*A. mento* possesses a pair of triangular quadrates (Fig. 4B, 9). The lateral and mesial condyles are connected with the angular of the lower jaw. Furthermore, the quadrate possesses a preopercular process featuring a groove that connects the quadrate with the preopercle (Fig. 9).


**Figure 10:** The main articulations of the suspensorium in *A. mento*: **(1)** between the palatine and the neurocranium, **(2a)**, **(2b)** between the hyomandibula and the neurocranium, **(3)** between the hyomandibula and the opercle, **(4)** between the quadrate and the lower jaw, **(5)** between the maxilla and the palatine.
**aa** = angulo-articular, **dn** = dental, **hm** = hyomandibular, **mx** = maxilla, **ncr** = neurocranium, **op** = opercular, **pmx** = premaxilla, **pt** = pterygoid, **qu** = quadrate, **sy** = symplectic.

The suspensorium complex shows five articulations (Fig. 10): (1) the palatine articulates with the anterior region of the neurocranium; (2a) and (2b) the hyomandibula articulates with the neurocranium on the otic region; (3) the posterior margin of the hyomandibula articulates with the opercular series; (4) the quadrate ventrally articulates with the angulo-articular; (5) the anterior region of the palatine articulates with the maxilla.

### 5.1.2.3 Hyoid apparatus

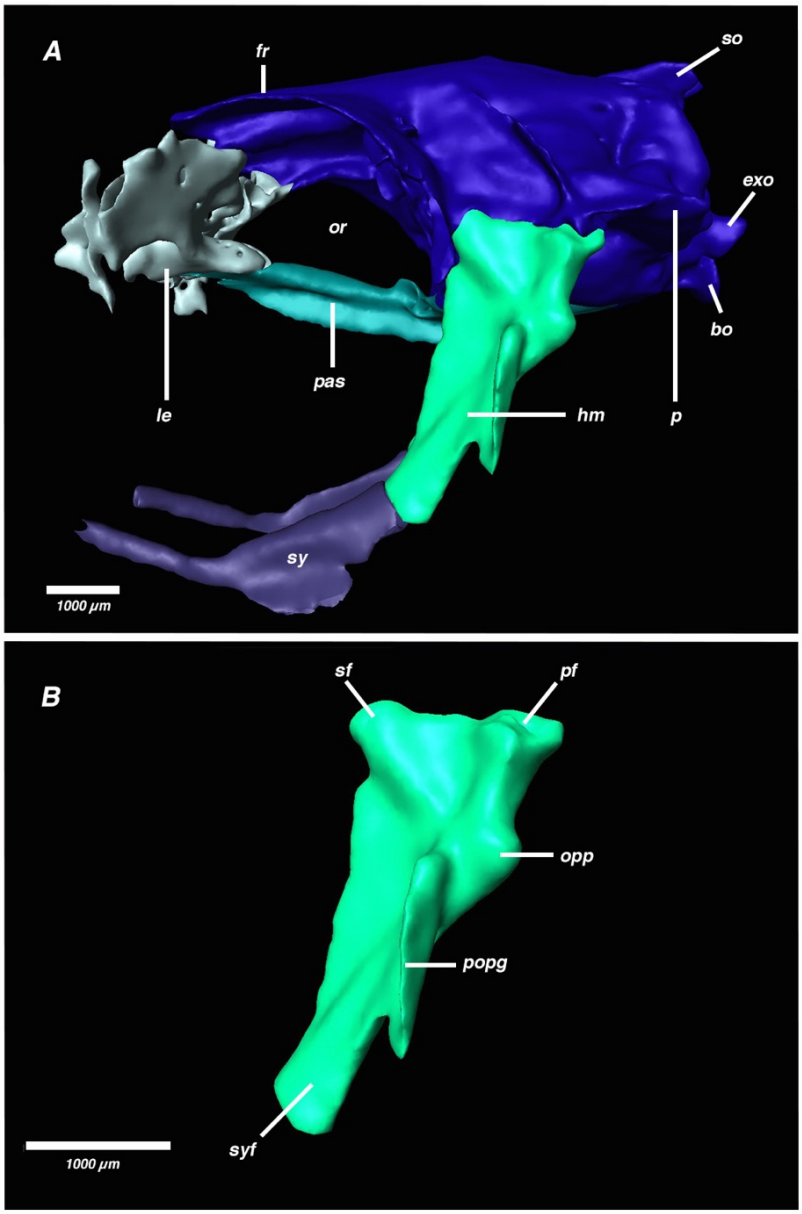


**Figure 11:** Lateral view of the neurocranium and the hyoid apparatus **(A)** of *Aphanius mento* and the hyomandibular in detail **(B)**. **bo** = basioccipital, **exo** = exoccipittal, **fr** = frontal, **hm** = hyomandibular, **le** = lateral ethmoid, **opp** = opercular process, **or** = orbit, **p** = pterotic, **pas** = parasphenoid, **pf** = pterotic facet, **popg** = preopercuar groove, **sf** = sphenotic facet, **so** = supraoccipital, **sy** = symplectic, **syf** = symplectic facet.

The symplectic, a bone that is present in teleostean fish, forms the ventral ossified element of the suspensorium. The paired hyomandibulars connect the symplectic to the neurocranial region, where they articulate with the hyomandibular fossa of the otic capsule (an excavation in the adjoined sphenotic, pterotic and prootic bones) (Fig. 11A). The ventral part of the hyomandibulars attaches to the quadrates via the so called symplectic, showing a symplectic facet (Fig. 11B). Thereby the symplectic builds a linkage between the jaw and the rest of the cranium. Furthermore, an opercular process as well as a preopercular groove connect the hyomandibular and the opercular region (Fig. 11B).

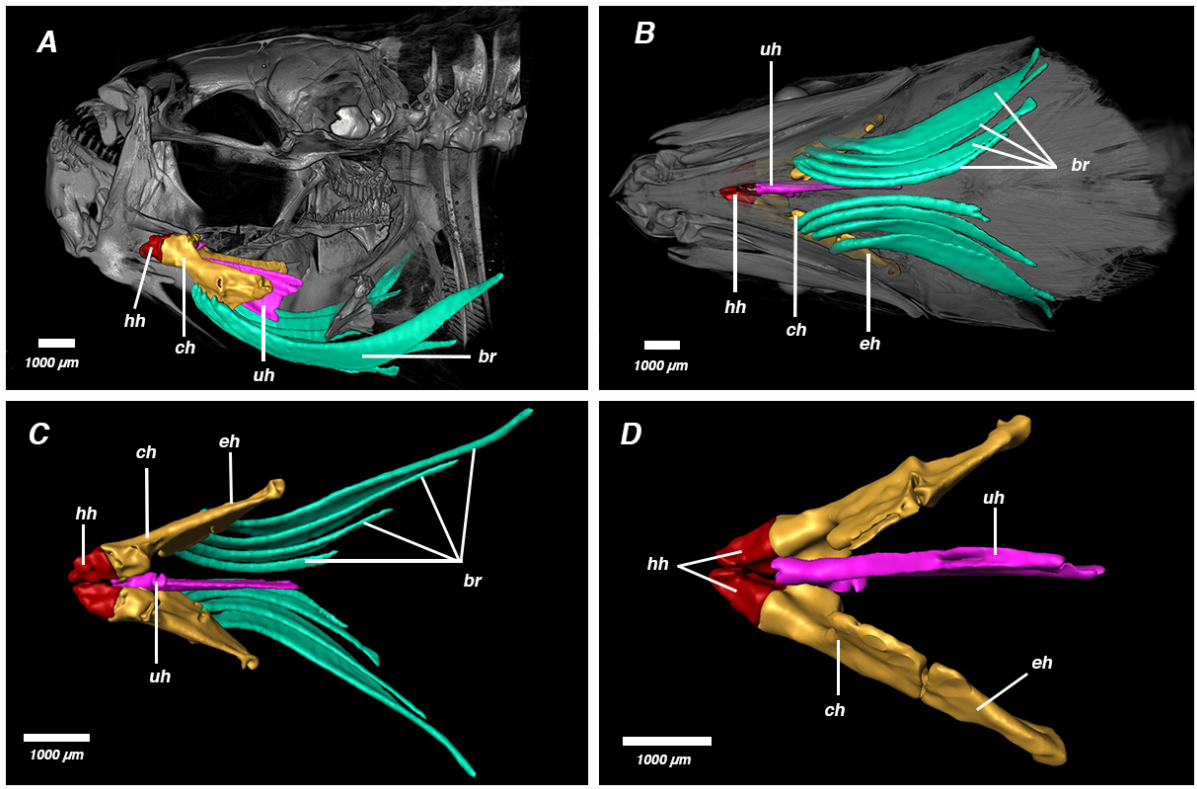


**Figure 12:** Medial view of the skeletal elements **(A)** and ventral view of both skeletal elements and musculature **(B)** of *Aphanius mento*, in combination with a reconstruction of the hyoid arch. Dorsal **(C)** and ventral **(D)** view of the reconstructed skeletal elements of the hyoid arch. **br** = branchiostegal rays, **ch** = ceratohyal, **eh** = epihyal, **hh** = hypohyal, **uh** = urohyal.

The hyoid arch comprises a small ventral hypohyal, a ceratohyal and an epihyal (Fig. 12A-D), as well as a basihyal (Fig. 14A/C/D, 15), which will be described later in this study. Together these ossified elements form the main movable unit of the hyoid, posterior to the lower jaw. Four pairs of curved branchiostegal rays join with the hyoid arch via the ceratohyal (Fig. 12A-C). The further posterior situated branchiostegal rays are generally larger and more elongated. Between the pair of ceratohyals lies the urohyal (Fig. 12A-D), an ossified “tendon bone” that originates in the septum between the longitudinal throat muscles. The urohyale and the anterior part of the hypohyale are connected via ligaments.

### 5.1.2.4 Opercular region

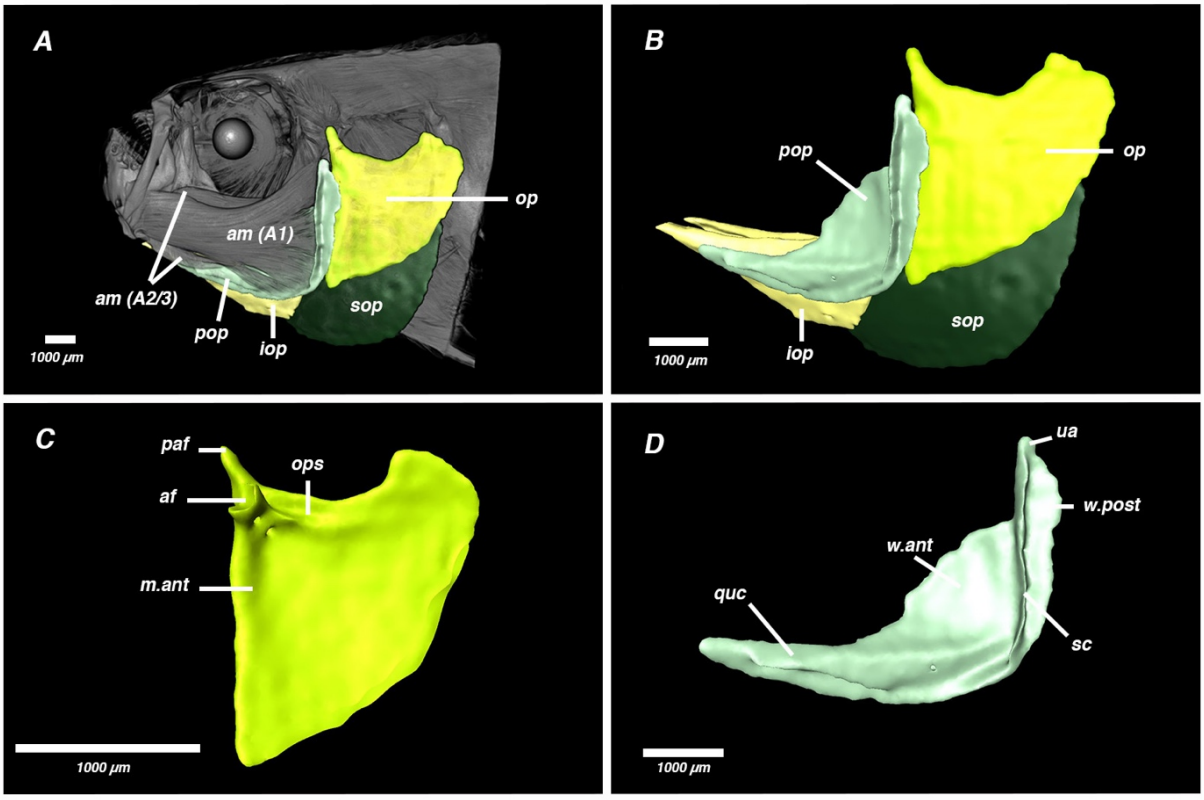


**Figure 13:** Lateral view of the skeletal elements and musculature in combination with the reconstructed opercular apparatus **(A)**, closeup of the reconstructed opercular apparatus **(B),** the inner side of the right opercle **(C)**, and the outer side of the preopercle **(D)** in detail. **am** = adductor mandibulae, **af** = articular fossa, **iop** = interopercle, **m.ant** = anterior margin, **op** = opercle, **ops** = opercular spine, **paf** = postarticular fossa, **pop** = preopercle, **quc** = quadrate crest, **sc** = sensory canal, **sop** = subopercle, **ua** = upper angle, **w.ant** = anterior wing, **w.post** = posterior wing.

The opercular apparatus consists of four pairs of flat dermal bones, covering the gills (Fig. 13A/B). These include the opercle, as well as, the inter-, pre- and subopercle, which is the innermost element (Fig. 13A/B).

The opercle is more or less rectangular and shows an opercular spine, as well as a postarticular fossa (Fig. 13C).

The preopercle is a paired bone, its upper arm (Fig. 13D) joins with the preopercular groove of the hyomandibular (Fig. 11B) to hold it in place. Its lower arm has a quadrate crest (Fig. 13D), that connects with the quadrate. The posterior wing of the preopercle (Fig. 13D) partially covers the opercle and subopercle (Fig. 13B).

### 5.1.2.5 Branchial arch

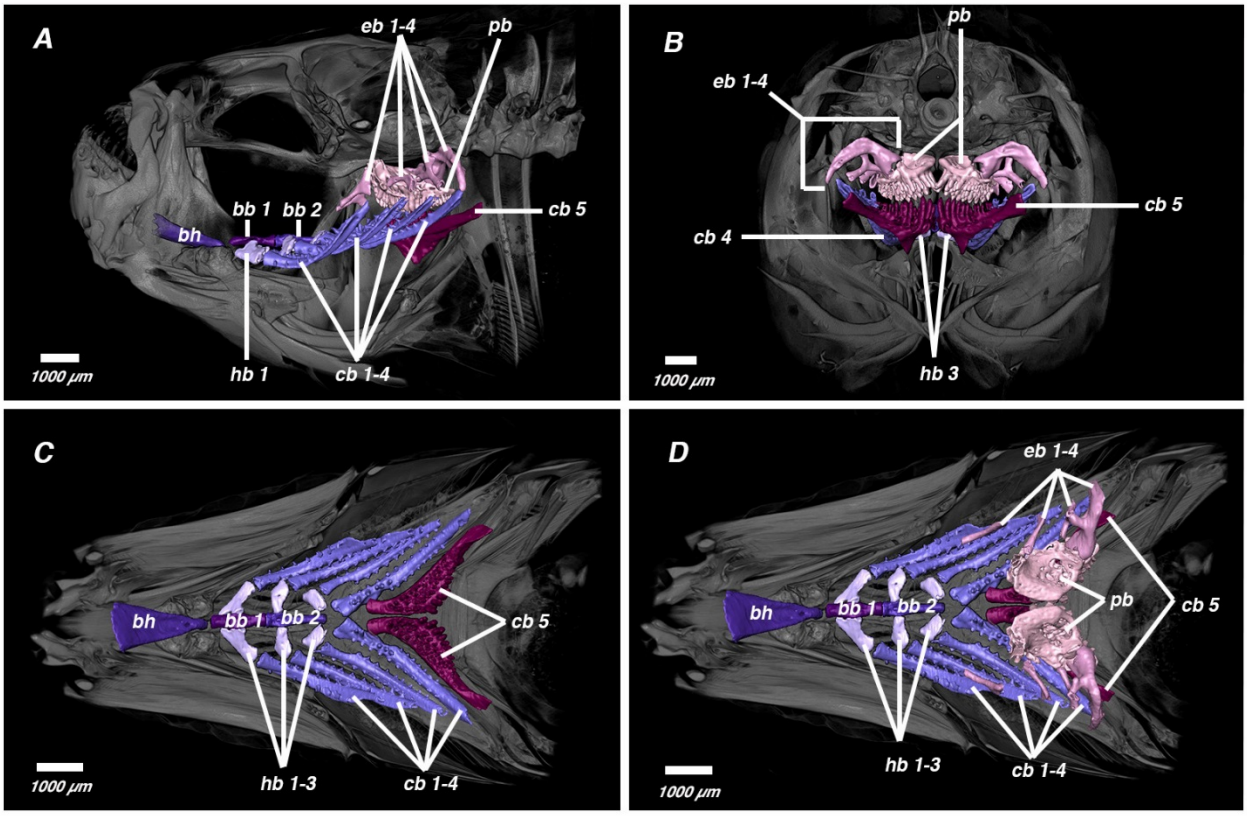


**Figure 14:** Lateral **(A)**, posterior **(B)** and dorsal **(C/D)** view of the branchial skeleton of *Aphanius mento*. **bb** = basibranchial, **bh** = basihyal, **cb** = ceratobranchial, **eb** = epibranchial, **hb** = hypobranchial, **pb** = pharyngobranchials.

The branchial complex includes four pairs of gill arches consisting of four pairs of gill rakers and pharyngeal tooth patches, which originally represented the fifth gill raker.

The basihyal is a bone that belongs to the hyoid arch. Nevertheless it has been included into the figures of the branchial arch to clarify the linkage between the basihyal (hyoid arch) and the basibranchials (branchial arch). The anterior part of the basihyal is cartilaginous (Fig. 15), while its posterior region consists of a bony element which is larger than the basibranchials (Fig. 14C/D).

The basibranchials form a chain from anterior to posterior. A largely ossified basibranchial 1 is positioned anterior to the second and third one (Fig. 14A/C/D). The third basibranchial is cartilaginous and therefore not visible in the reconstructions of the skeletal element of the branchial arch. It is positioned posterior to the basibranchial 2 and can be vaguely discerned in Fig. 15. The basibranchials are bordered laterally by cartilaginous heads of the hypobranchials 1 to 3 (Fig. 15). The fourth hypobranchial is cartilaginous and positioned between the last basibranchial and the fourth ceratobranchial. The ossified hypobranchials 1 to 3 are elongated and trapezoid (Fig. 14C/D). Furthermore, they are surrounded by cartilage along their lateral and

posterior borders. There are five pair of toothed and mostly ossified ceratobranchials present (Fig. 14A/C/D). The fifth ceratobranchials expand posteromedially supporting the lower pharyngeal tooth plate with conical shaped teeth that are arranged in four to five rows, building the lower pharyngeal jaw (LPJ) (Fig. 14B/C/D). Furthermore, the branchial skeleton consists of four pairs of epibranchials (Fig. 14A/B/D). The fourth epibranchial is, in comparison to the other epibranchials, fairly big and therefore supports the pharyngobranchials almost alone. They are largely ossified, except for their cartilaginous endpoints. In contrast to the ceratobranchials, the epibranchials bear no teeth (Fig. 14A/B/D). In addition, the fourth pair of epibranchials show an uncinate process (Fig. 14D). The ossified pharyngobranchials 1-4 are merged, giving support to the upper pharyngeal tooth plate, bearing robust conical teeth arranged in four to five rows (Fig. 14A/B/D). So, the upper pharyngeal jaw (UPJ) consists of the pharyngobranchials, which are placed beside the cartilaginous tips of the epibranchials 2, 3 and 4 (Fig. 14D).

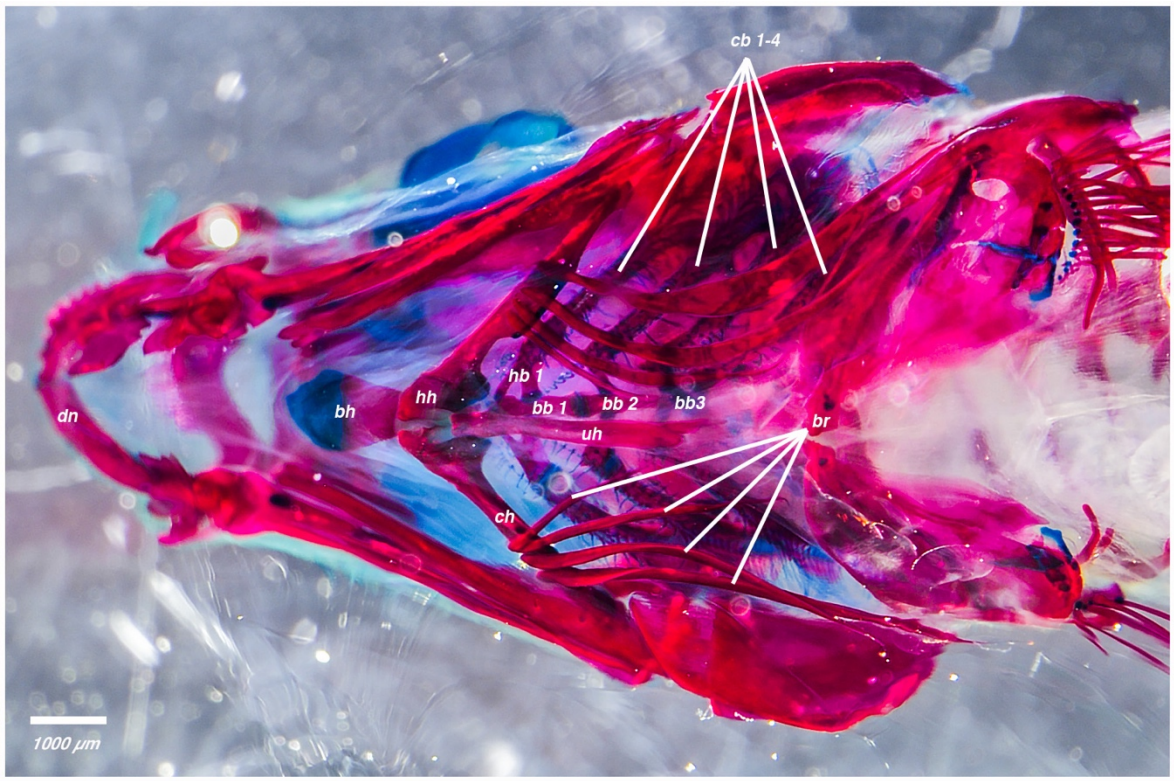


**Figure 15:** Ventral view of *Aphanius mento*. The bony elements are stained red and the cartilaginous elements are stained blue. **bb** = basibranchial, **bh** = basihyal, **br** = branchiostegal rays, **ch** = ceratohyal, **dn** = dental, **hb** = hypobranchial, **hh** = hypohyal.

### 5.1.3 Pectoral girdle

In *Aphanius mento* the cleithrum arches form the dorsolateral side of the head toward the branchiostegal rays (Fig. 1). They connect the cranium to the pectoral and pelvic fins via the posttemporal and the supracleithrum. The posttemporal is V-shaped and builds two connections with the neurocranial region (Fig. 1).

## 5.2 Cranial musculature

### 5.2.1 Ocular muscles

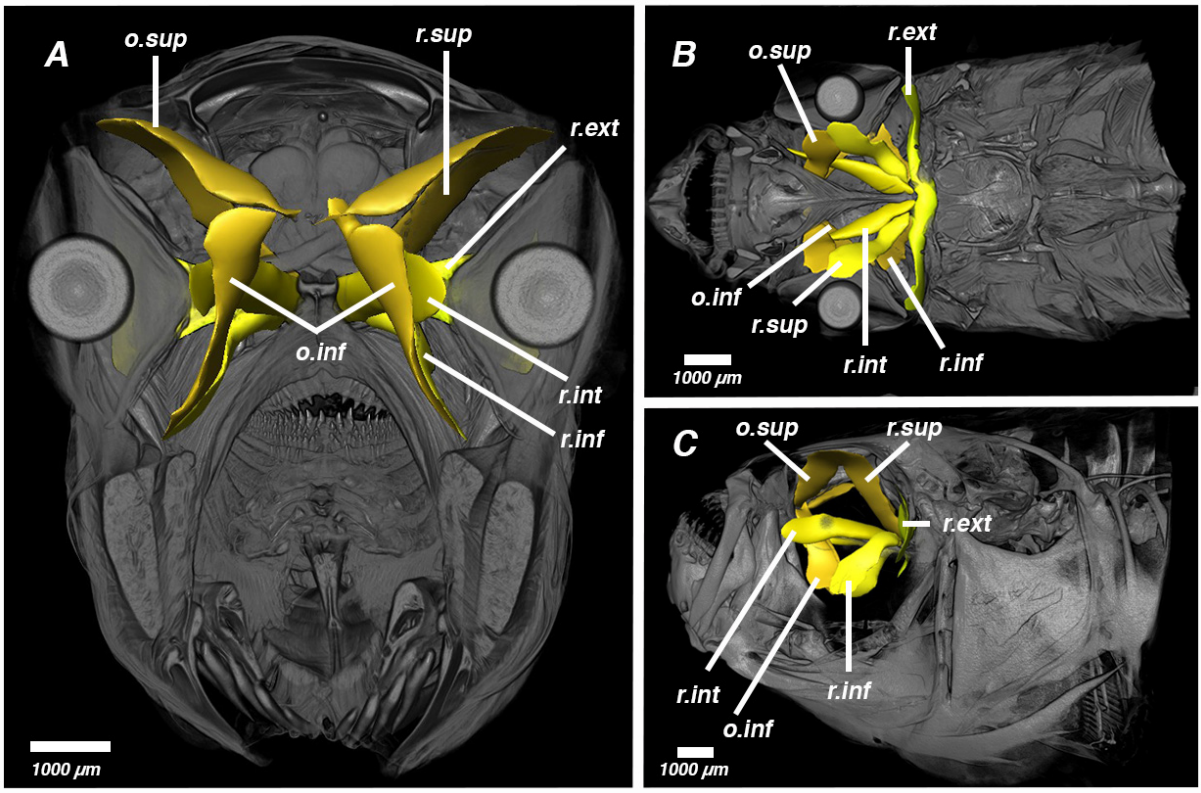


**Figure 16:** Anterior **(A)**, dorsal **(B)** and lateral view of *Aphanius mento*, showing the reconstructed extraocular muscles. **o.inf** = oblique extraocular inferior, **o.sup** = oblique extraocular superior, **r.ext** = rectus extraocular externus, **r.inf** = rectus extraocular inferior, **r.int** = rectus extraocular internus, **r.sup** = rectus extraocular superior.

Fig. 16A-C shows three pairs of extraocular muscles: inferior and superior oblique; inferior and superior rectus; and external and internal rectus. At the ventral side of the *A. mento* eye the inferior rectus and inferior oblique overlap (Fig. 16A/C). A similar overlap of the superior oblique and superior rectus muscles takes place on the dorsal side of the eye (Fig. 16A-C).

## 5.2.2 Mandibular muscles

Fig. 17A shows a microCT scan of the musculature of *Aphanius mento* including some skeletal elements and the reconstruction of all three adductor mandibulae muscles (A1-A3), Fig. 17B the skeletal elements and musculature including the reconstruction of two adductor mandibulae muscles (A2/A3). There are two branches of the first division of the A1: A1α and A1β (Fig. 18A-D). A1α is larger than A1β, and its fibres proceed horizontally from their origin on the hyomandibula and preopercle to their attachment site on the posterior end of the maxilla.

In contrast to A1α, the anterior part of A1β inserts on the maxilla as well as the premaxilla.

A large part of A2 originates from the suspensorium and inserts on ligamentous tissue that covers the ventral part of the premaxilla and further seems to be attached to the dentary (Fig. 18A-D).

A3 is the smallest of the three adductor mandibulae muscles (Fig 17A/B). Its anterior region attaches on the premaxilla as well as the angulo-articular. The posterior region of A3 attaches laterally on the quadrate.

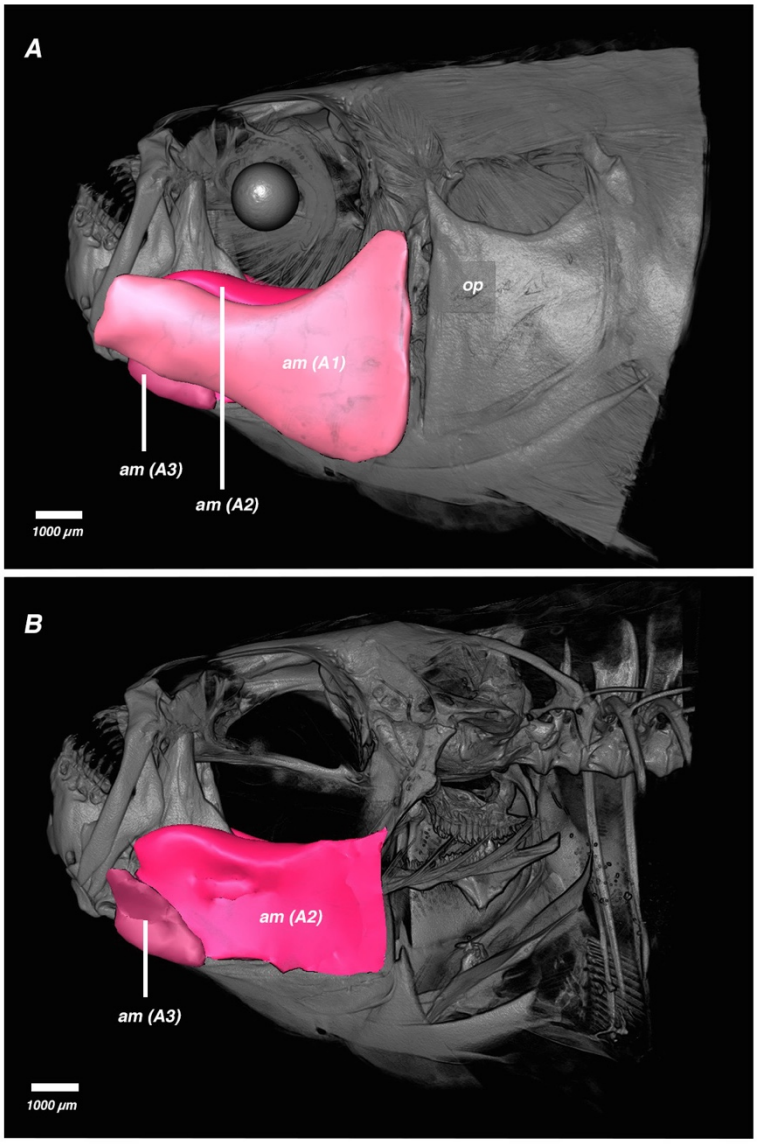


**Figure 17:** Lateral view of skeletal elements and musculature, including all three adductor muscles **(A)** and the lateral view of just the skeletal elements in combination with the reconstructed muscles **(B)** in *Aphanius mento*. **am** = adductor mandibulae.

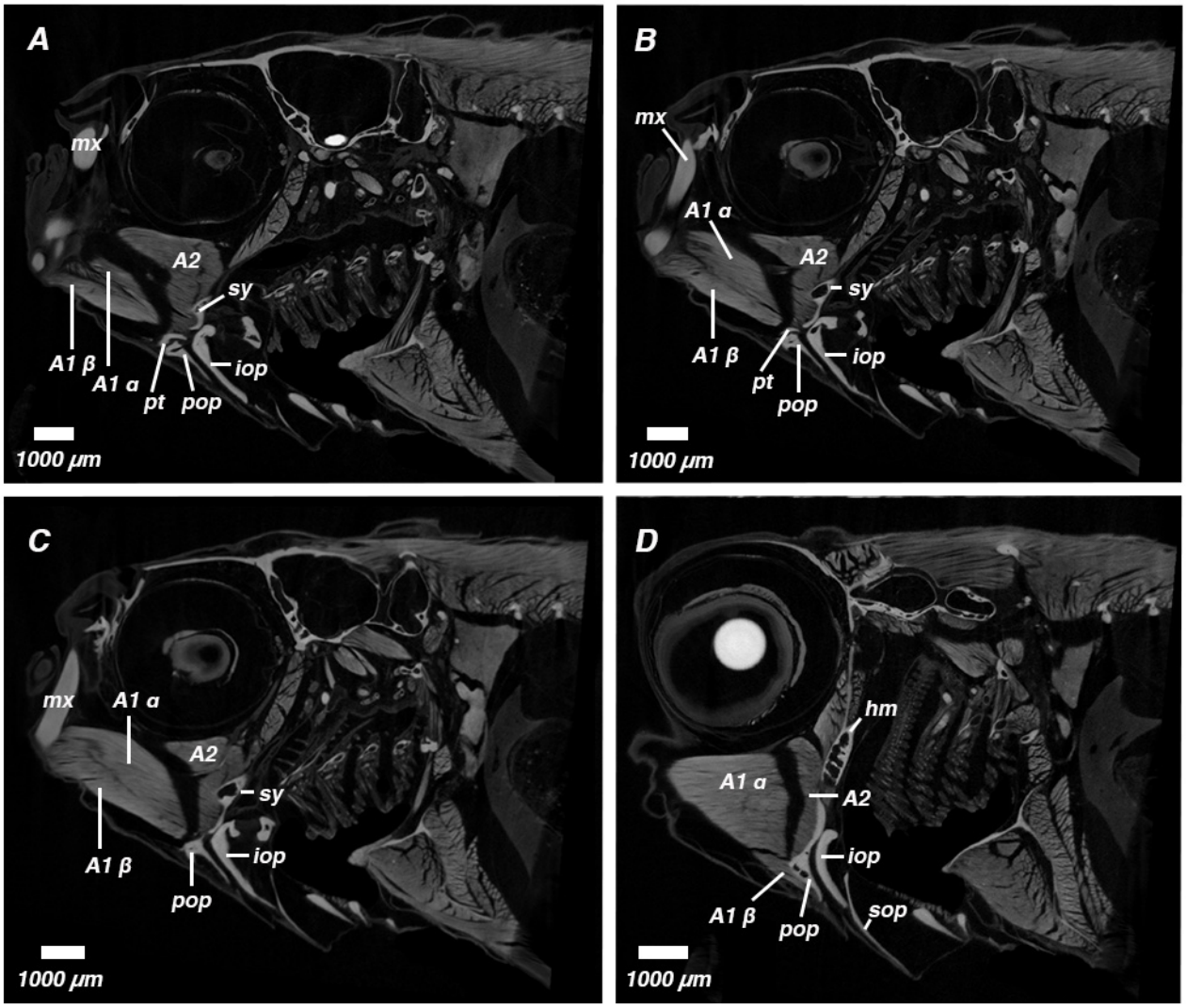


**Figure 18:** Selected parasagittal microCT slices of *Aphanius mento*, showing skeletal elements and musculature. from the most median **(A)** to the most lateral situated slice **(D)**. The focus lays on the divided adductor mandibulae muscles as well as the skeletal elements surrounding them. **A1α** and **A1β** are both subdivisions of **A1** (main adductor mandibulae). **A2** is another subdivision of the whole adductor mandibulae complex. **hm** = hyomandibular, **iop** = interopercular, **mx** = maxilla, **pop** = preopercular, **pt** = pterygoid, **sop** = subopercular, **sy** = symplectic.

Table 1 summarizes the attachment sites and function of the muscles A1, A2, and A3.

**Table 1:** Attachment sites and function of the mandibular muscles in *Aphanius mento*.

| MUSCLE | ORIGIN | INSERTION | FUNCTION |
|---|---|---|---|
| Adductor mandibulae 1 (A1) | • hyomandibula<br>• preopercle | • posterior end of the maxilla | • holds maxilla in place during feeding<br>• closes mouth |
| Adductor mandibulae 2 (A2) | • hyomandibula<br>• preopercle | • ligamentous tissue<br>• dentary | • closes mouth<br>• assists adducting suspensorium |
| Adductor mandibulae 3 (A3) | • lateral side of the quadrate | • premaxilla as well as the angulo-articular | • closes mouth<br>• assists adducting suspensorium |

## 5.2.3 Hyoid muscles

The hyoid muscles include the arcus palatini musculature, the adductor, dilatator and levator operculi, the hyoid abductor and adductor and many more.

**Table 2:** Attachment sites and function of the hyoid muscles in *Aphanius mento*.

| MUSCLE | ORIGIN | INSERTION | FUNCTION |
|---|---|---|---|
| Adductor arcus palatini anterior | • parasphenoid | • pterygoid<br>• hyomandibula | • raises the suspensorium |
| Adductor arcus palatini posterior | • neurocranium | • hyomandibula | • raises the suspensorium |
| Adductor operculi | • ventral side of the pterotic of the neurocranium | • dorsal part of opercle | • adducts opercles |
| Dilatator operculi | • orbit | • anterodorsal tip of opercle | • moves opercles apart and expands the gill cavity |
| Hyohyoideus abductors | • hypohyals<br>• anterior ceratohyals (hyoid arch) | • branchiostegal rays<br>• mesial aponeurosis, meeting its contralateral counterpart | • expand the branchiostegal membrane |
| Hyohyoideus adductors | • mesial aponeurosis, meeting its contralateral counterpart | • branchiostegal rays | • constrict the branchiostegal membrane |
| Hyohyoideus inferior | • hypohyals<br>• ceratohyals | • urohyal<br>• anterior region of branchiostegal rays | • adduction of the hyoid arch |
| Intermandibularis | • dentary (left side) | • dentary (right side) | • joins the two mandibles |

| | | | |
|---|---|---|---|
| Levator arcus palatini | • neurocranium | • hyomandibula | • lifts the palatal arch<br>• increases buccal volume<br>• suspensorial elevation/abduction |
| Levator operculi | • lateral side of the pterotic of the neurocranium | • dorsal part of opercle | • may interfere in lower jaw depression through the interoperculo-mandibular ligament<br>• abducts opercles |
| Protractor hyoideus | • dentary | • hyoid arch | • mainly elevates hyoid bars, and depresses mandible (mouth opening)<br>• pulls hypobranchial system forward |
| Sternohyoideus | • pectoral girdle | • urohyal | • pulls the hyobranchial system backwards<br>• plays a major role in hyoid depression, and, through a series of mechanical linkages, in mouth opening and suspensorial abduction |

### 5.2.3.1 Palatinal musculature

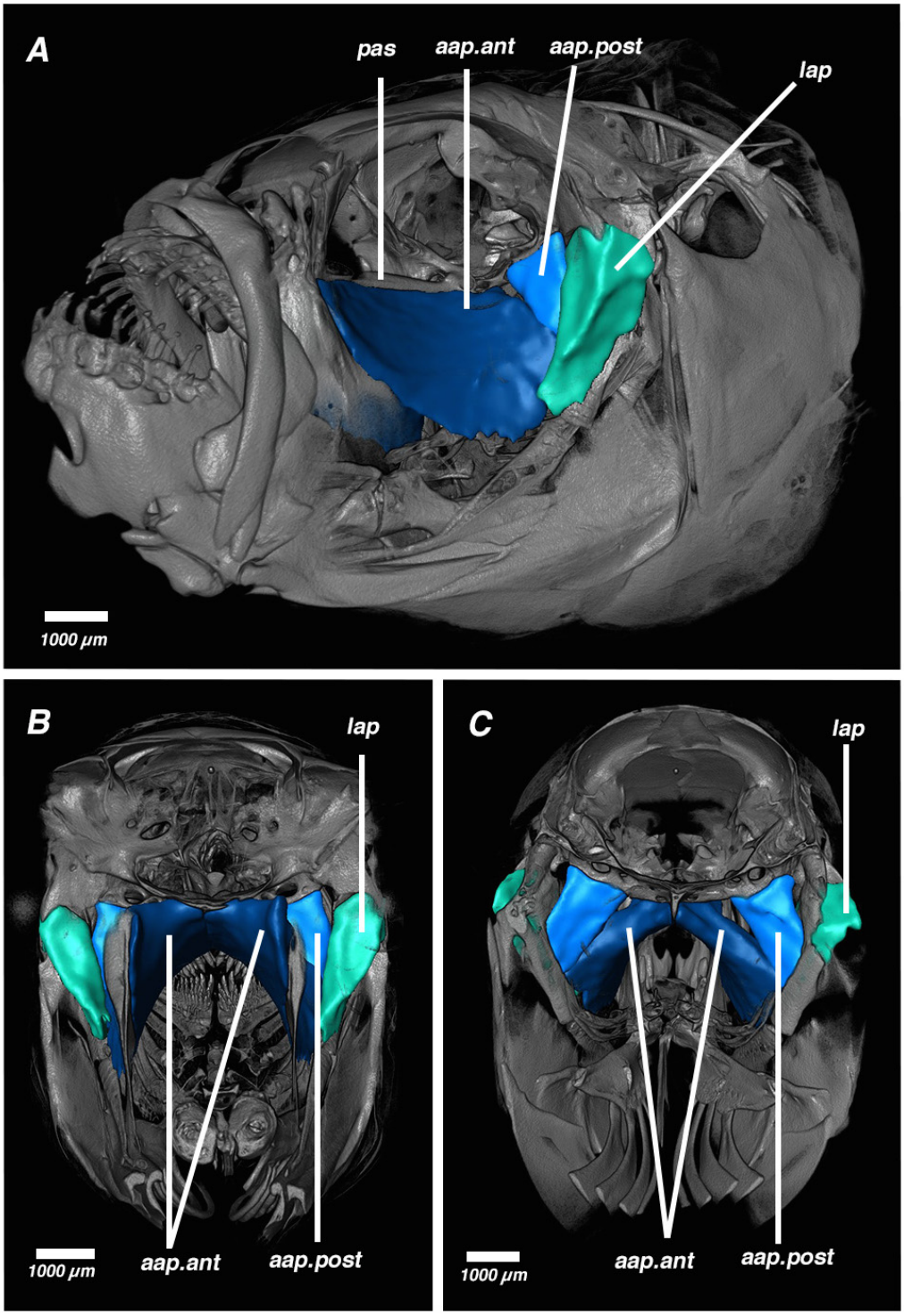


**Figure 19:** Lateral **(A)**, anterior **(B)** and posterior **(C)** view of *Aphanius mento*, showing the reconstructed palatine musculature. **aap.ant** = adductor arcus palatini anterior, **aap.post** = adductor arcus palatini posterior, **lap** = levator arcus palatini, **pas** = parasphenoid.

Two superficial and sequential muscles are present, the levator arcus palatini, with attachment sites at neurocranium and along the hyomandibula on the suspensorium (Fig. 19A-C, 20) (anteriorly), and the dilatator operculi (posteriorly) between the rear of the orbit and the

posterodorsal tip of the opercle (Fig. 20). Right below the levator arcus palatini and the hyomandibular articulations with the neurocranium lies the posterior positioned part of the adductor arcus palatine, coloured in a lighter blue than the rest of the adductor arcus palatini (Fig. 19A-C). The anterior part of this muscle originates from the ventrolateral margin of the parasphenoid, where it expands anteriorly and therefore underlies the orbit (Fig. 19A-C, 20).

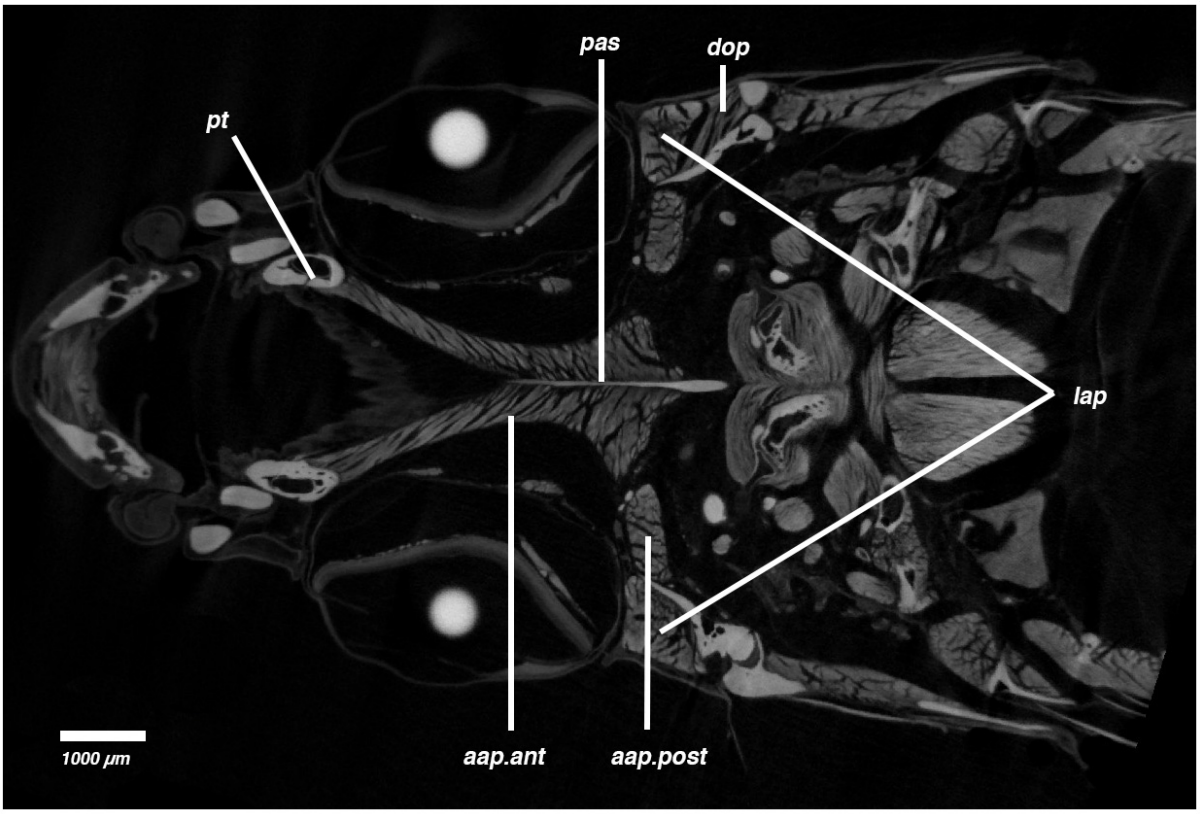


**Figure 20:** Frontal microCT slice of *Aphanius mento* showing skeletal elements and musculature of the head region. **aap.ant** = adductor arcus palatini anterior, **aap.post** = adductor arcus palatini posterior, **dop** = dilatator operculi, **lap** = levator arcus palatini, **pas** = paraspenoid, **pt** = pterygoid.

### 5.2.3.2 Opercular musculature

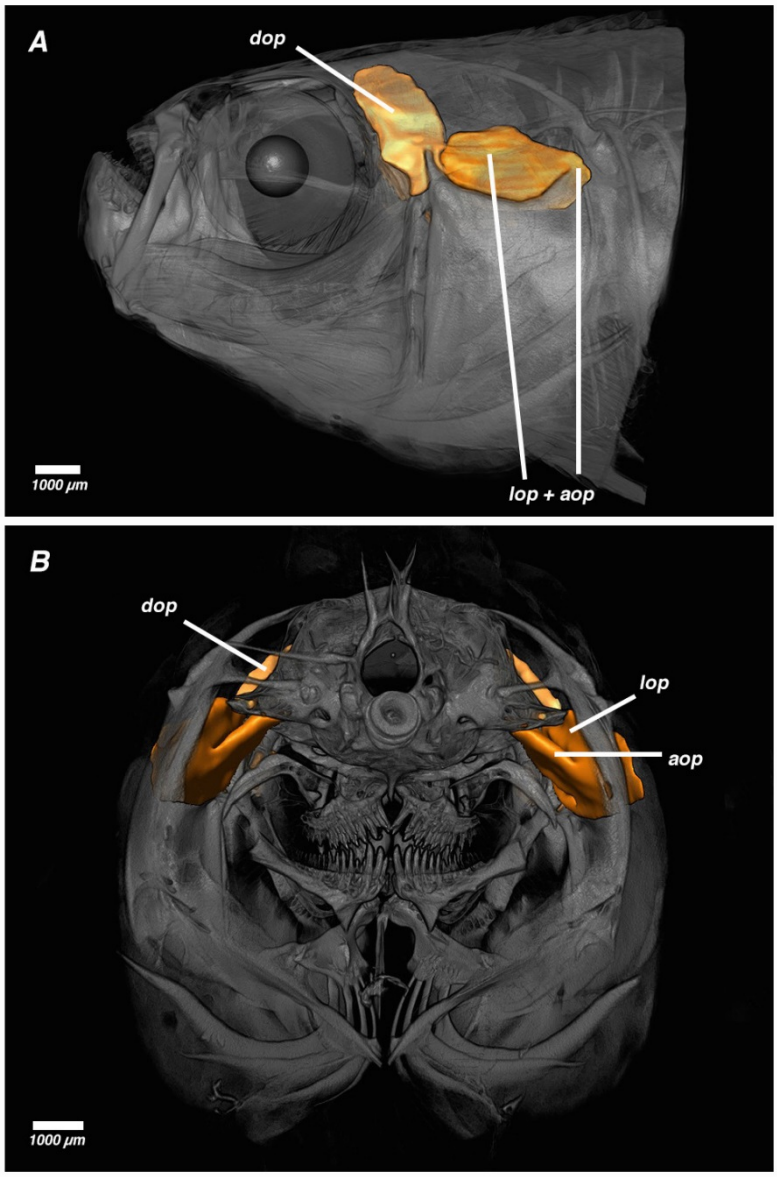


**Figure 21:** Lateral **(A)** and posterior **(B)** view of *Aphanius mento*, showing micro CT scans in combination with the reconstructed adductor, dilatator and levator operculi. **aop** = adductor operculi, **dop** = dilatator operculi, **lop** = levator operculi.

Fig. 21A shows a lateral view of the opercular musculature *in A. mento*. Due to the way the muscle fibers merge, it is difficult to differentiate between the levator and adductor operculi from this perspective. The dilatator operculi runs between the orbit and the anterodorsal tip of the opercle. Posterior to the dilatator operculi, the levator operculi and the adductor operculi muscle can be found (Fig. 21A/B). Both originate at the pterotic of the neurocranium and attach at the dorsal part of the opercular. The adductor operculi originates on the ventral side of the pterotic, while the levator operculi originates on the lateral side of the pterotic (Fig. 21B).

### 5.2.3.3 Ventral hyoid musculature

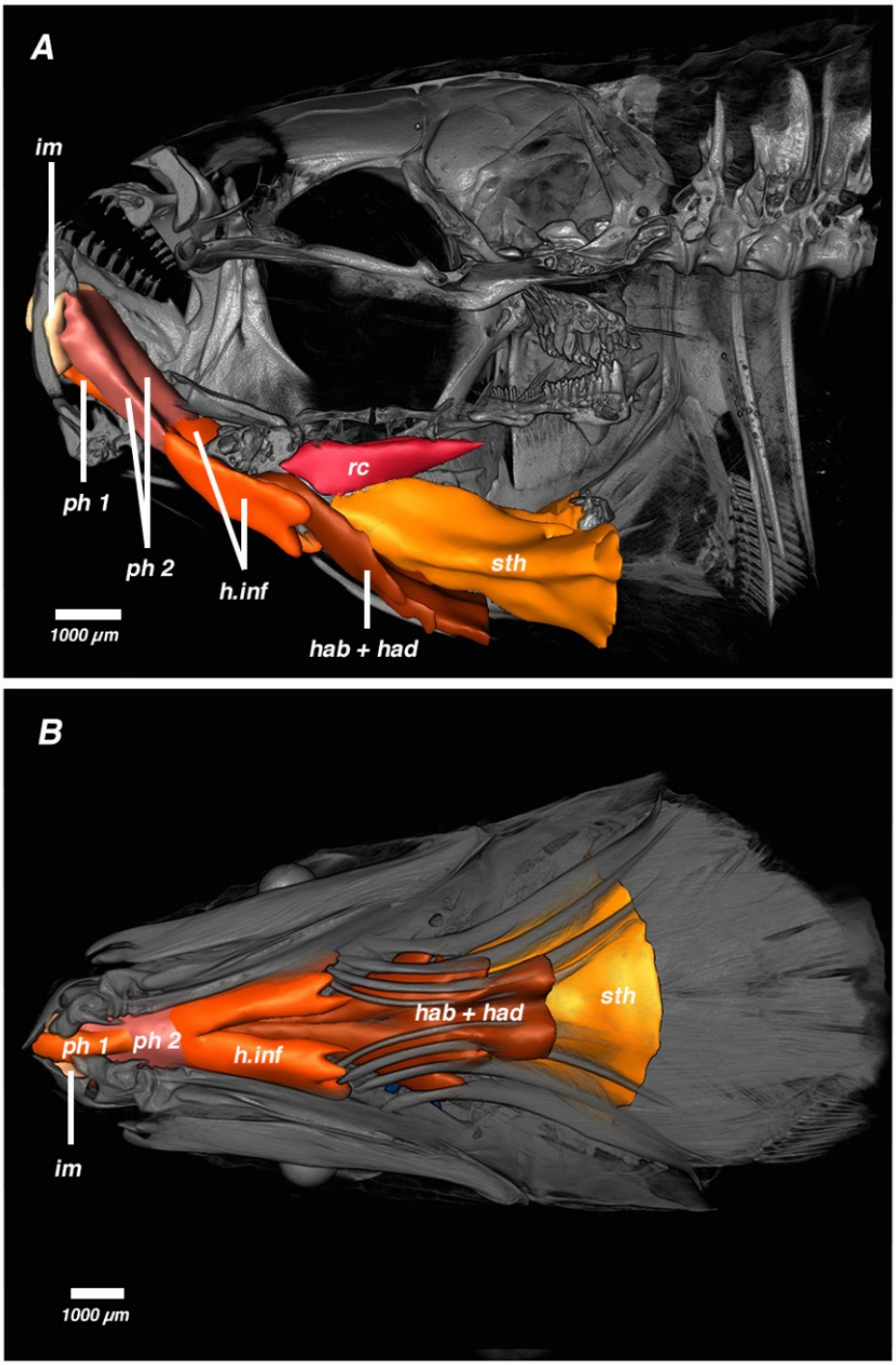


**Figure 22:** Medial view of the skeletal elements **(A)** and ventral view of both skeletal elements and musculature **(B)**, of *Aphanius mento*, combined with the reconstruction of the hyoid musculature and the rectus communis. **hab** = hyohyoideus abductors, **had** = hyohyoideus adductors, **h.inf** = hyohyoideus inferior, **im** = intermandibularis, **ph** = protractor hyoideus, **rc** = rectus communis, **sth** = sternohyoideus.

The musculus sternohyoideus is connected to the urohyal (Fig. 22A) and the pectoral girdle. This muscle doesn't belong to the hyoid musculature. It is the only hypobranchial muscle in *A. mento*. The hyohyoideus inferior muscle originates from the anterior region of the ceratohyals

as well as the hypohyals and inserts at the urohyal and the anterior region of the branchiostegal rays (Fig. 22A/B). So this muscle connects the ceratohyal and the branchiostegal rays on the one hand (Fig. 22B) and the dentary on the other hand (Fig. 22A). The hyohyoideus abductors also connect the anterior ceratohyals and hypohyals with the branchistegal rays, and are further connected to the hyohyoideus adductors. While the hyohyoideus abductors insert on a mesial aponeurosis, the hyohyoideus adductors originate from this mesial aponeurosis.

In the anterior region, the protractor hyoideus is divided into a dorsal (ph 2) and a ventral (ph 1) part (Fig. 22A/B). Between those two subdivisions the intermandibularis muscle is positioned. The fibres of the intermandibularis stretch transversely between the two halves of the dentaries (Fig. 22A).

## 5.2.4 Branchial muscles

The branchial musculature includes a variety of muscles attached to the skeletal elements of the branchial arch. The following table shows the attachment sites of these branchial muscles in *A. mento*, as well as their functions.

**Table 3:** Attachment sites and function of the branchial muscles in *Aphanius mento*.

| MUSCLE | ORIGIN | INSERTION | FUNCTION |
|---|---|---|---|
| Adductores branchiales (1-4) | • ceratobranchials (1-4) | • epibranchials (1-4) | • pull epibranchials and ceratobranchials towards each other |
| Adductor branchialis 5 | • lateral tip of ceratobranchial 4 | • lateral tip of ceratobranchial 5 | • pulls ceratobranchials 4 and 5 towards each other |
| Levator externus (1-4) | • prootic region (neurocranium) | • epibranchials (1-4) | • lift the UPJs<br>• protract the UPJs |
| Levator internus (2-3) | • prootic muscular crest (neurocranium) | • merged pharyngobranchials | • lift the UPJs<br>• protract the UPJs<br>• pull the UPJs apart |
| Levator posterior | • posterolateral tip of the pterotic | • epibranchial 4 | • lifts the epibranchial 4 |
| Obliquus dorsalis | • merged pharyngobranchials | • epibranchials (3-4) | • flexes the joint between the epibranchials and the merged pharyngobranchials |
| Obliquus posterior | • epibranchial 4 | • ceratobranchial 5 | • works as a levator of the fifth ceratobranchial |
| Obliquus ventrales (1-3) | • hypobranchials (1-3) | • ceratobranchials (1-3) | • play a role in adjusting the position and movement of |

| | | | |
|---|---|---|---|
| | | | the pharyngeal teeth during the feeding and respiratory cycle |
| Rectus communis | • urohyal | • ceratobranchial 5 | • lowers the LPJs |
| Retractor dorsalis | • ventral surface of the first vertebrae | • merged pharyngobranchials | • lifts and pulls each UPJ backward<br>• antagonist to the levator complex |
| Rectus ventrales (2-4) | • hypobranchials (1-3) | • ceratobranchials (2-4) | • play a role in adjusting the position and movement of the pharyngeal teeth during the feeding and respiratory cycle |
| Transversus dorsalis anterior | • fascia in the dorsal midline | • merged pharyngobranchials (both sides) | • joins the two merged pharyngobranchials |
| Transversus dorsalis posterior | • fascia in the dorsal midline | • epibranchial 4 (both sides) | • joins the two epibranchials 4 |
| Transversus ventralis 4 | • base ceratobranchial 4 (both sides) | • base ceratobranchial 5 (both sides) | • rotates LPJs axially so that the teeth are properly turned towards the skull<br>• helps to stabilize the lower jaw elements into a single functional structure |
| Transversus ventralis 5 | • posterior region of ceratobranchial 5 (left side) | • posterior region of ceratobranchial 5 (right side) | • brings the LPJs toward each other<br>• helps to stabilize the lower jaw elements into a single functional structure |

### 5.2.4.1 Levator externus/internus

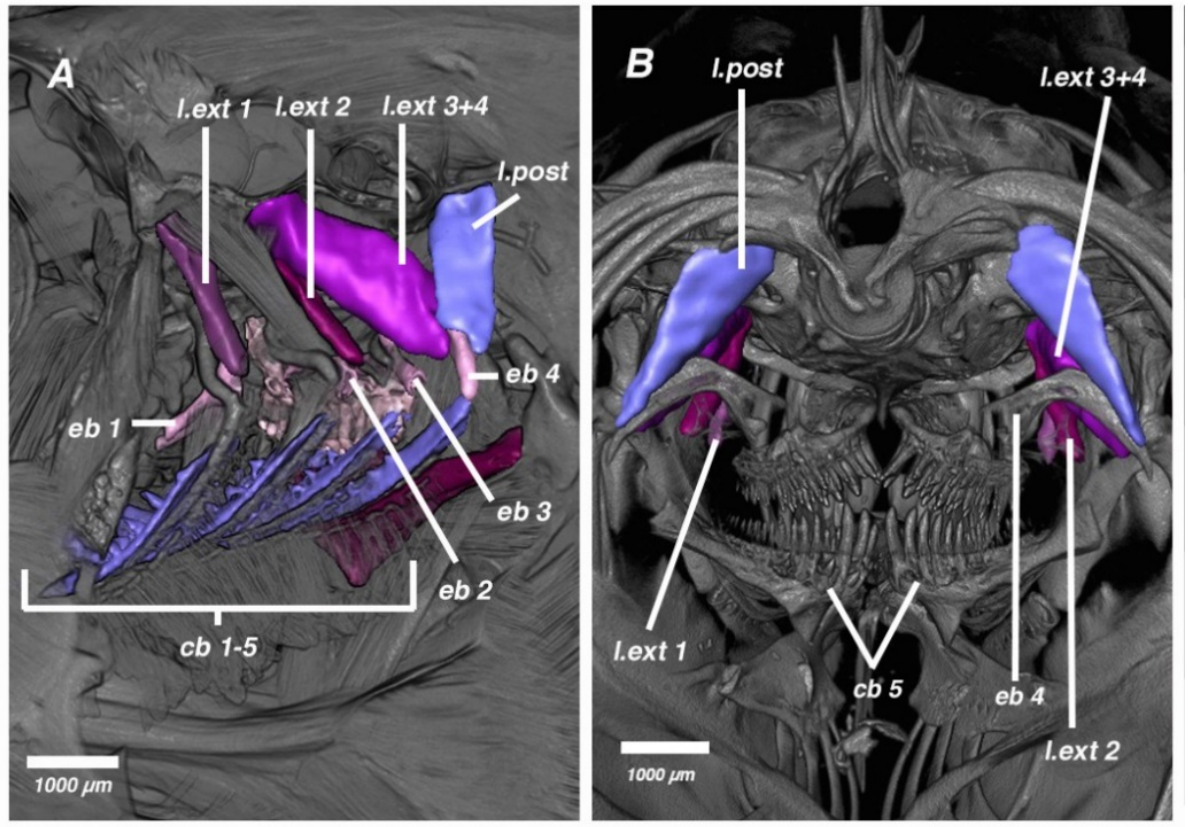


**Figure 23:** Lateral closeup **(A)** and posterior view **(B)** view of the external levator muscles of *Aphanius mento*. **cb** = ceratobranchial, **eb** = epibranchial, **l.ext.** = levator externus**, l.post.** = levator posterior.

Four external levator muscles connect the four epibranchial elements with the neurocranium (Fig. 23A/B, 25B). The third and fourth external levators are partially fused and therefore difficult to differentiate. The levator posterior muscle also connects the fourth epibranchial to the neurocranium (Fig. 23A/B, 25A/B).

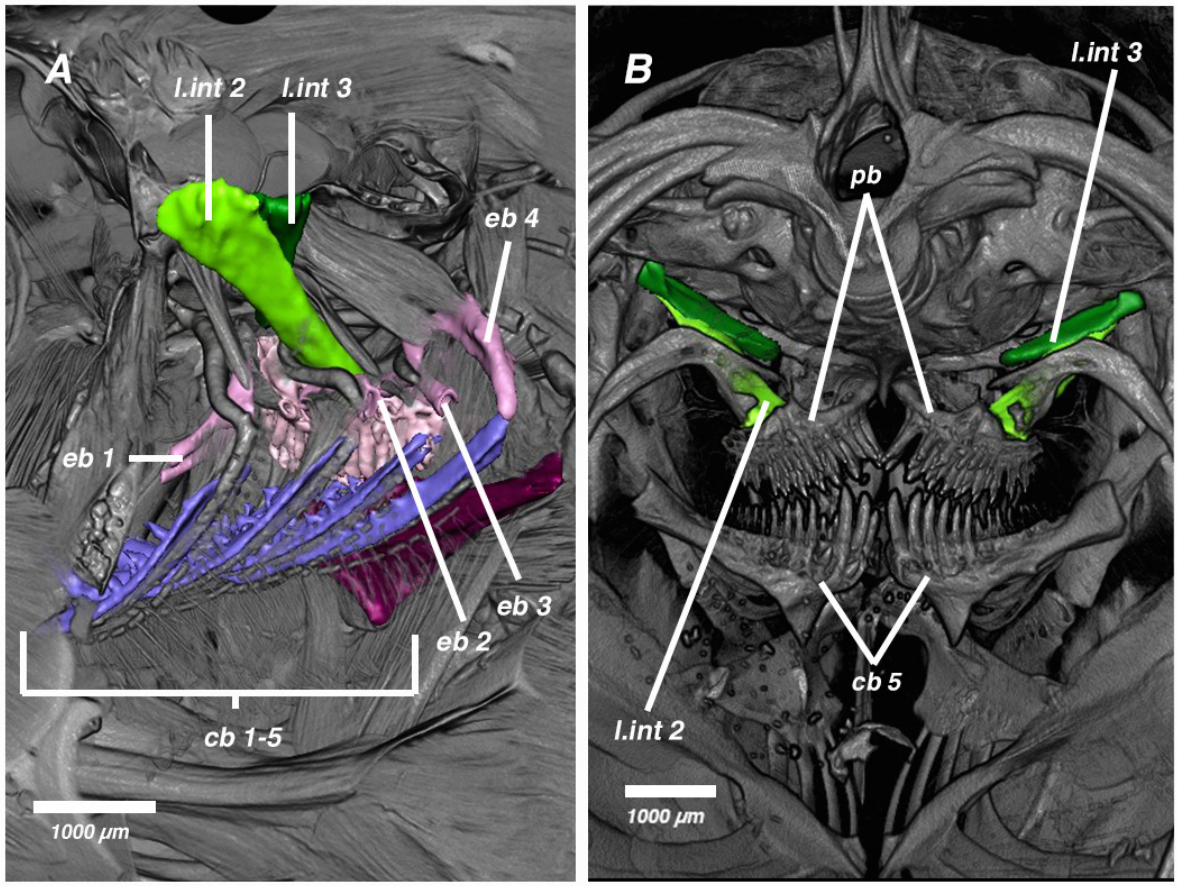


**Figure 24:** Lateral closeup **(A)** and posterior view **(B)** of the internal levator muscles of *Aphanius mento*. **cb** = ceratobranchial, **eb** = epibranchial, **l.int.** = levator internus, **pb** = pharyngobranchial.

Furthermore, two internal levators extend from the pharyngobranchial to the neurocranial base (Fig. 24A/B). Both the external and internal levator muscles extend in a rostrodorsal direction towards the neurocranium (Fig. 23A/B, Fig. 24A/B).

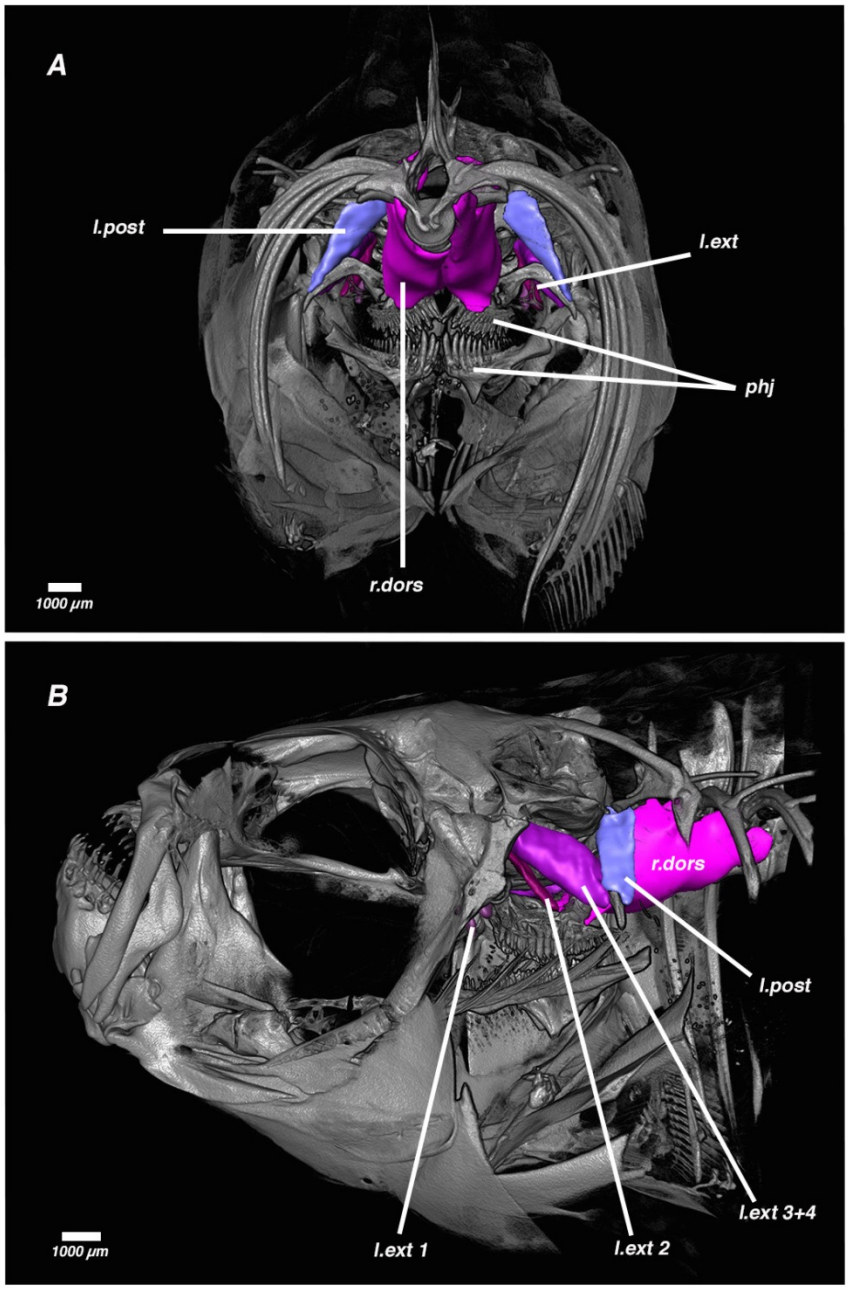


**Figure 25:** Posterior **(A)** and lateral **(B)** view of *Aphanius mento*, showing the external levator muscles in combination with the retractor dorsalis. **l.ext** = levator externus, **l.post** = levator posterior**, phj** = pharyngeal jaws, **r.dors** = retractor dorsalis.

The very prominent retractor dorsalis muscle inserts on the UPJ consisting of the pharyngo-branchial elements, and extends to the ventral side of the neurocranium as well as the ventral side of the anterior vertebrae (Fig. 25A/B).

### 5.2.4.2 Transversus dorsalis

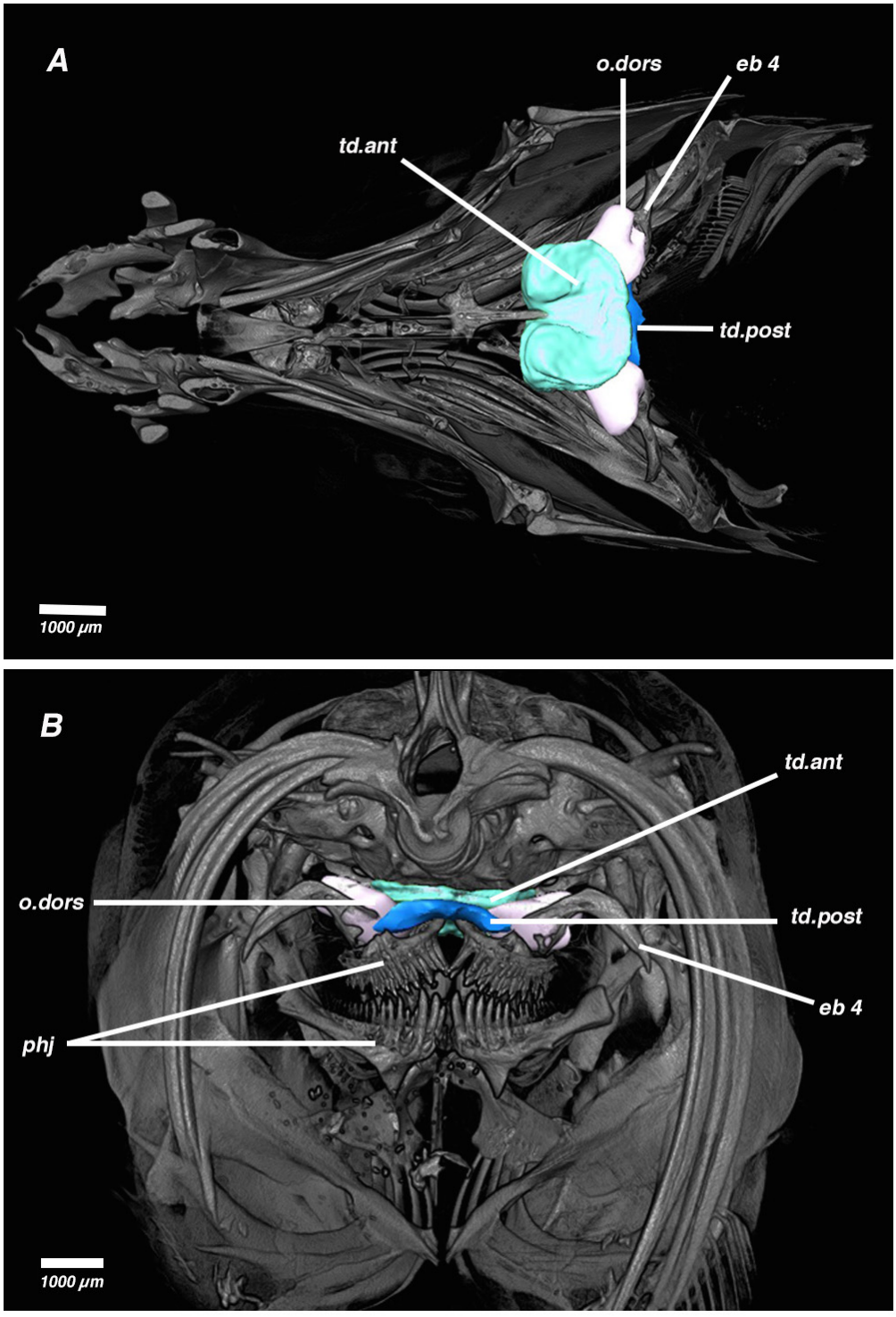


**Figure 26:** Dorsal **(A)** and posterior **(B)** view of *Aphanius mento*, showing the pharyngeal jaws as well as obliquus dorsalis, transversus dorsalis anterior and transversus dorsalis posterior. **eb** = epibranchial, **o.dors** = obliquus dorsalis, **phj** = pharyngeal jaws, **td.ant** = transversus dorsalis anterior, **td.post** = transversus dorsalis posterior.

In Fig. 26A, the dorsal region has been removed to show the two transversus dorsalis muscles and the obliquus dorsalis. The transversus dorsalis muscles connect the left and right pharyngeal elements which build the upper pharyngeal jaw. These muscles stretch from a fascia in the

dorsal midline to the branchial arches and can be separated into transversus dorsalis anterior and tranversus dorsalis posterior (Fig. 26A/B). The latter runs between the fourth left and right epibranchials. The obliquus dorsalis muscle connects the pharyngobranchial and epibranchial 4 dorsally (Fig. 26A/B). The microCT slice in Fig. 27 shows the fibre course of the musculature in the region of the transversus dorsalis muscles and the retractor dorsalis.

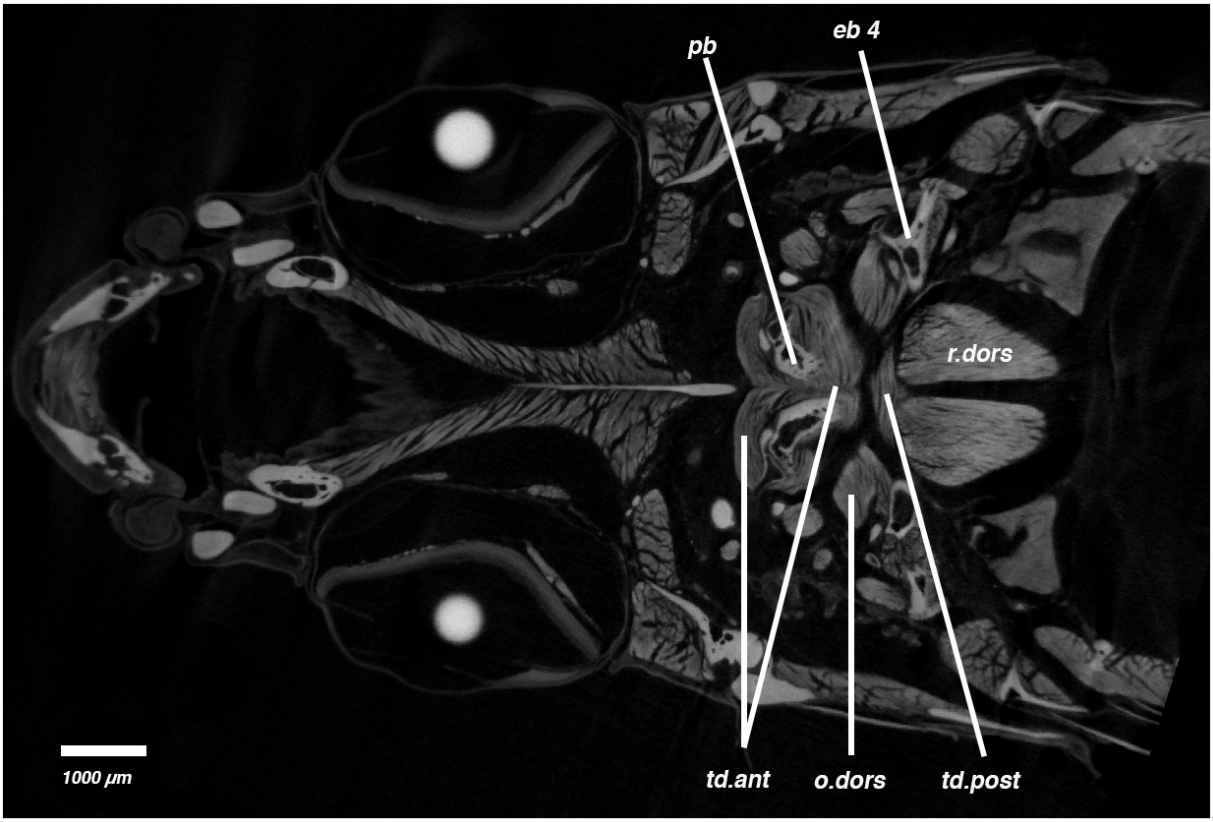


**Figure 27:** Frontal microCT slice of *Aphanius mento* showing skeletal elements and musculature of the head region. **eb** = epibranchial, **o.dors** = obliquus dorsalis, **pb** = pharyngobranchial, **r.dors** = retractor dorsalis, **td.ant** = transversus dorsalis anerior, **td.post** = transversus dorsalis posterior.

### 5.2.4.3 Ventral branchial musculature

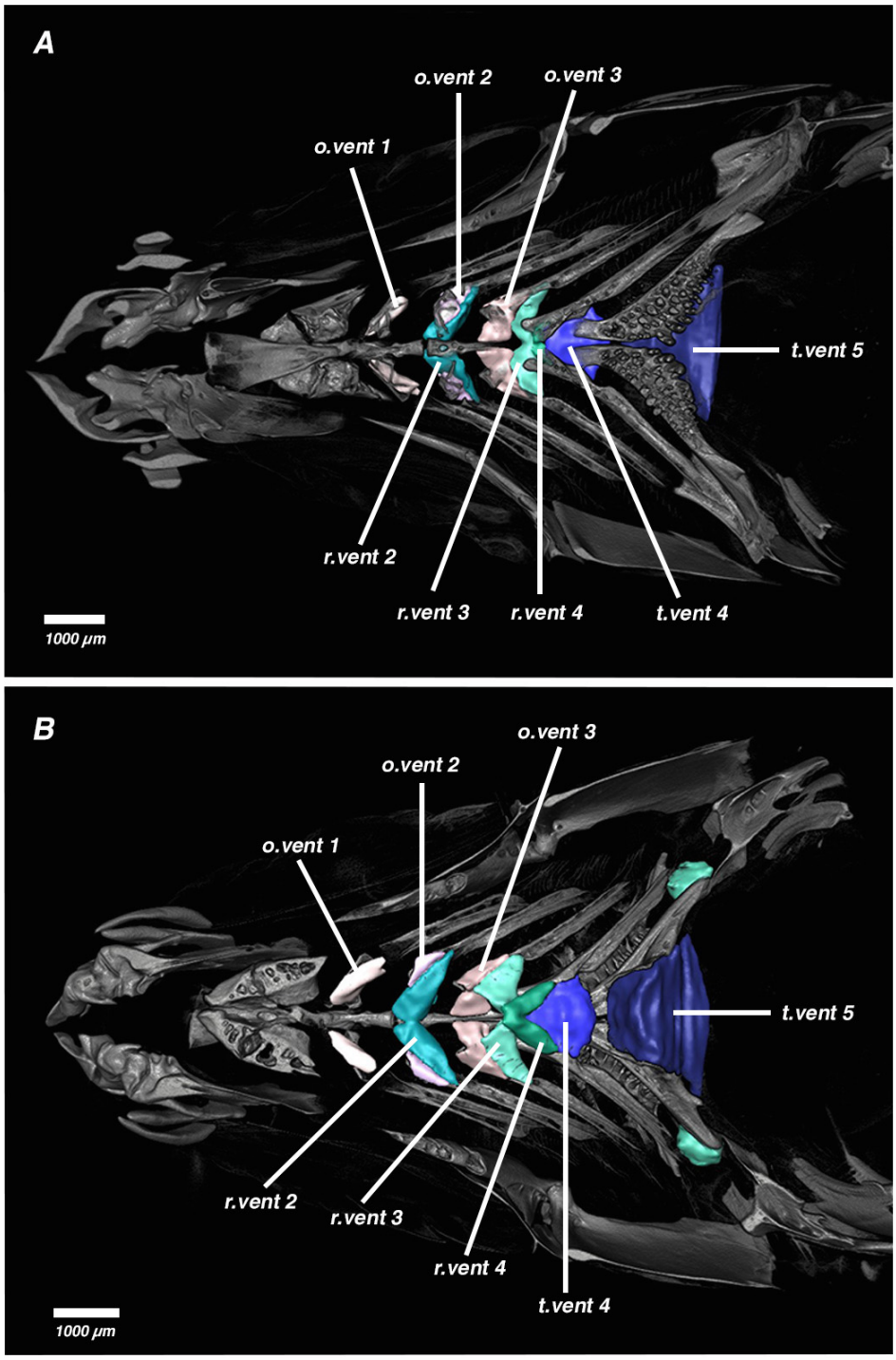


**Figure 28:** Dorsal **(A)** and ventral **(B)** view of microCT scans showing the branchial region of *Aphanius mento* and the reconstructions of the ventral branchial musculature. **o.vent** = obliquus ventralis, **r.vent** = rectus ventralis, **t.vent** = transversus ventralis.

As shown in Fig. 28A and Fig. 28B, the ventral parts of the gill arches in *A. mento* have three obliqui ventrales (o.vent 1-3). These muscles connect the hypobranchial and ceratobranchial elements of the first three branchial arches. The pharyngeal apparatus also includes two transversi ventrales (t.vent 4-5), as well as three recti ventrales (r.vent 2-4). The transversi ventrales

bridge the gap between the fourth and fifth ceratobranchials. The three recti ventrales connect a ceratobranchial element with the preceding hypobranchial element (Fig. 28A/B).

Another member of the branchial musculature is the rectus communis (Fig. 22A). The anterior part of this muscle is attached to the urohyal, while the posterior part inserts at the ceratobranchial 5.

### 5.2.4.4 Adductor branchialis

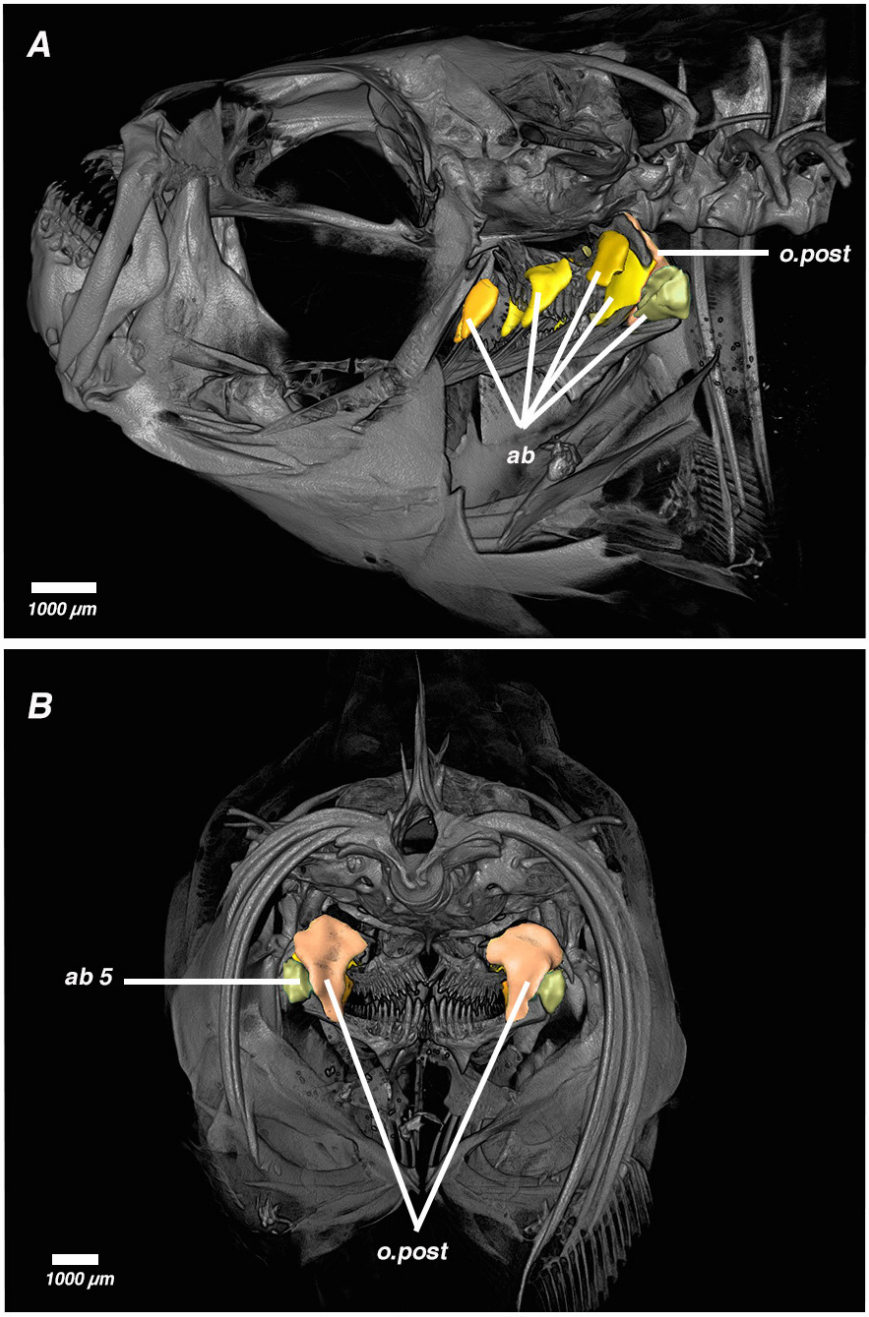


**Figure 29:** Lateral **(A)** and posterior **(B)** view of *Aphanius mento*, showing the adductor branchialis muscles and the obliquus posterior. **ab** = adductor branchialis, **o.post** = obliquus posterior.

Fig. 29A shows a microCT scan of the skeletal elements of *Aphanius mento*'s head region in combination with the adductor branchialis muscles, which connect each ceratobranchial with the epibranchial of the same arch, except for the fifth one. The fifth adductor connects the ceratobranchials 4 and 5 (Fig. 29A/B). However, fibers of the adductor branchialis 5 may extend onto the cartilaginous end of epibranchial 4 at its joint with ceratobranchial 4. The obliquus posterior connects the fifth ceratobranchial and the fourth epibranchial (Fig. 29A/B).

## 5.3 Pectoral girdle musculature

**Table 4:** Attachment sites and function of the musculature of the pectoral girdle in *Aphanius mento*.

| MUSCLE | ORIGIN | INSERTION | FUNCTION |
|---|---|---|---|
| levator pectoralis | • posteroventrolateral region of the skull | • pectoral girdle | • elevates the pectoral girdle |
| Pharyngo-clavicularis externus | • ventral region of ceratobranchial 5 | • pectoral girdle | • draw the LPJs downward |
| Pharyngo-clavicularis internus | • posterior region of ceratobranchial 5 | • pectoral girdle | • draws the LPJs backward |
| protractor pectoralis | • neurocranium | • pectoral girdle | • protracts the pectoral girdle |

### 5.3.1 Pharyngoclavicularis

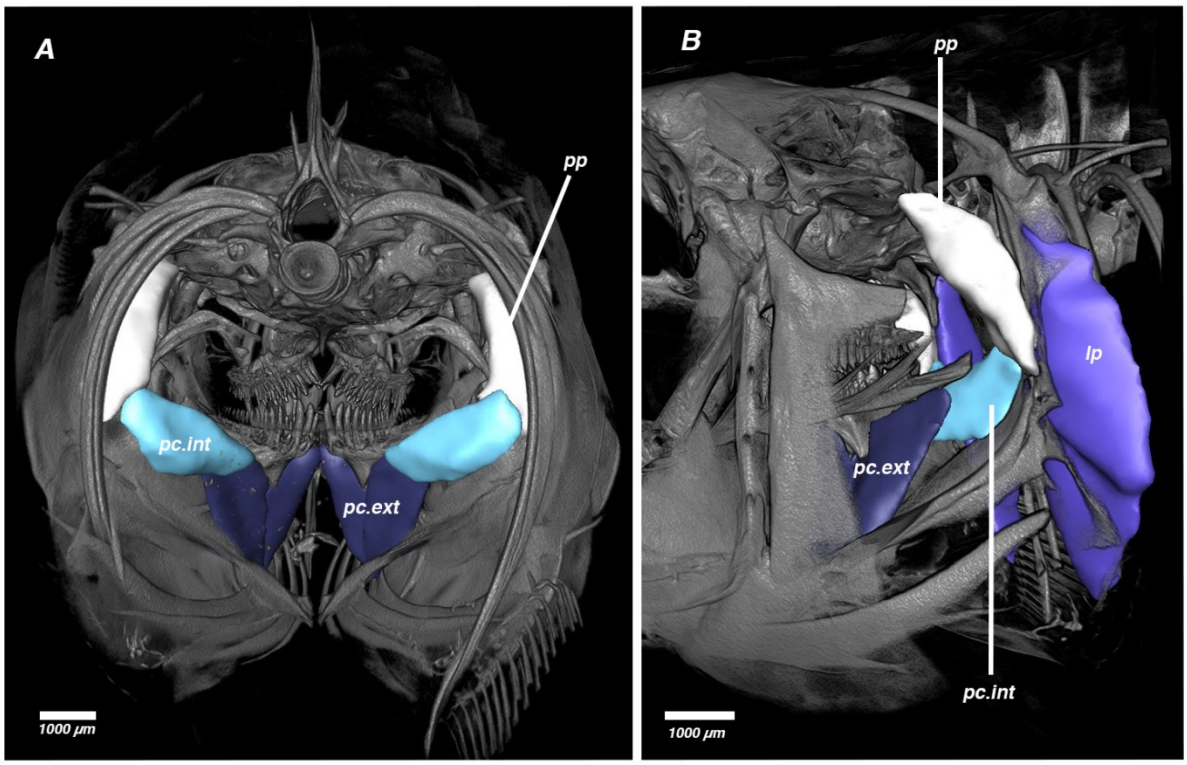


**Figure 30:** Posterior **(A)**, and lateral **(B)** view of the head region of *Aphanius mento*. Both show skeletal elements in combination with the reconstructed pharyngo-clavicularis internus and externus as well as the protractor pectoralis and the levator pectoralis. **lp** = levator pectoralis, **pc.ext** = pharyngo-clavicularis externus, **pc.int** = pharyngo-clavicularis internus, **pp** = protractor pectoralis.

The fifth ceratobranchials are connected ventrally and posteriorly to the pectoral girdle by the pharyngo-clavicularis internus and the split externus muscles (Fig. 30A/B). The protractor pectoralis muscle connects the neurocranium with the pectoral girdle. The levator pectoralis originates from the posteroventrolateral region of the skull and lies posterolateral to the protractor pectoralis (Fig. 30A/B).

# Discussion

How the skull of an animal is built is strongly influenced by its lifestyle. It has to be adapted to a variety of prey and habitats, and therefore the skull exhibits considerable diversity to accompany diverse feeding mechanisms (Smith, 1993; Kardong, 2012).
In this study, the head region of the cyprinodontid *Aphanius mento* has been studied in order to investigate the cranial bones and muscles important for feeding.
In teleosts there are several couplings and interactions of cranial bones and muscles during feeding. A network of connections and muscle actions function in three aspects of feeding, namely mouth opening, premaxillary protrusion and suction generation (Westneat, 2006).

The differentiation of cartilaginous elements was difficult due to the lack of information provided by the microCT scans. Thus, as a second technique clearing and staining was used. Although the cartilage was made visible by blue staining, it was still hard to determine the exact position of some cartilaginous elements (for example the rostral cartilages), due to the fact that the skeletal elements have been cross-dyed.
Furthermore, the size of the reconstructed muscles can differ from their original size due to the preparation of the specimen prior to microCT-scanning or the process of surface smoothing during reconstruction in Amira.

## 5.4 Skull and jaws

The **skull** of an actinopterygian fish consists of several important movable blocks of bones that play a role in prey capture (Westneat, 2006).
It can be divided into two main regions: the **neurocranium** and the **splanchnocranium** (i.e. visceral cranium) (Huby and Parmentier, 2019).
While the neurocranium protects the brain and sensory organs, the visceral cranium supports the jaws and gills and offers attachment sites for the respiratory as well as the feeding muscles (Huby and Parmentier, 2019).

### 5.4.1 Neurocranium

The **neurocranium** in *A. mento* persists of numerous bony elements (Fig. 1) and can be divided into four main regions: the olfactory region, the orbital region, the otic region and the occipital region (Helfman et al., 2009; Huby and Parmentier, 2019).

It serves as a supporting structure for other mechanical units and provides direct support and protection to the brain and the sensory organs, as well as the **otoliths** (Michel et al., 2014).

Otoliths, also known as "ear stones", are found in the head of all fishes, excluding sharks, rays and lampreys. The inner ear of bony fish normally consists of 3 otolith pairs (Helfman et al, 2009), the sagittal, the asteriscal, and the lapillar (Fig. 3A). The sagitta is generally the largest and the asteriscus the smallest out of the three. This is also the case in *A. mento*.

Otoliths serve different functions, for example gravity detection and magnetic reception (Helfman et al, 2009). The sagitta and asteriscus respond to inertia and sound stimulus, and collectively the otoliths provide sensory input. This arrangement is crucial for orientation and balance in the water column, as well as for detecting sound (Caillet et al., 1986).

Otoliths can differ in shape and size and are unique to a species. They enlarge at a rate similar to that of body growth. This can be seen in their concentric rings that correspond to slower and faster growth rates over the year. These rings can be used to estimate the age of a fish (Helfman et al, 2009).

Because the saccular otoliths in *Aphanius* are usually species specific, and vary in size and contour, they provide an important data set of morphological characters and therefore present a valuable tool for taxonomy and analyses of species diversity (Schulz-Mirbach et al., 2006; Reichenbacher et al., 2009).

Below the neurocranium lies the cross-shaped parasphenoid, a further skeletal element (Fig. 3A/B). It represents the only dermal bone in the basicranial region. It joins with the vomer anteriorly, forms the posteroventral base of the skull and further plays a role during feeding, as it acts as a hard palate (Helfman et al., 2009).

## 5.4.2 Splanchnocranium

The **splanchnocranium** also consists of three regions: the oromandibular region, the hyoid region and the branchial region (Helfman et al., 2009; Kardong, 2012; Huby and Parmentier, 2019).

The most anterior arch becomes the mandibular arch, followed by the hyomandibula and the suspensorium that support the jaws. Further posterior a branchial basket which supports the gill arches and filaments is present (Vandewalle et al., 1995, 2000; Parmentier et al., 1998; Engeman et al. 2009; Carvalho and Vari, 2015).

### 5.4.2.1 Oral jaws

Primitive teleosts display a small **premaxilla** that is anterior in position. Both premaxilla and **maxilla** bear teeth, but the major tooth bearing bone is the maxilla. As the teleostei evolved, the premaxilla began to elongate and overlap the maxilla. At one point the premaxilla fully excludes the maxilla from the gape of the mouth and becomes the only tooth-bearing element of the upper jaw (Schaeffer and Rosen, 1961; Motta, 1984) (Fig. 4A-C, 5, 6). In the most highly evolved teleost fish such as cyprinodontiformes, the premaxilla develops an "ascending process" (Westneat, 2006). This process extends upward and backward to overlap the snout region of the head, as found in *A. mento* (Fig. 4A, 6). It increases the mobility of the jaw by forcing the premaxilla forward into a protruded position (Westneat, 2006). The upper jaw in *A. mento* persists of a paired maxilla that is located above the premaxilla (Fig. 4A-C,6,7). In contrast to ancestral teleosts such as Elopidae, Albulidae, Anguilliformes, Clupeidae and Engraulidae, whose maxillae tend to bear teeth (Gregory, 1933), *A. mento* has toothless maxillae (Fig. 4A-C, 5, 6). The ascending arm of each maxilla is more complex, featuring an external and internal process and a premaxillary sulcus (Fig. 5). The dorsal elements of the premaxillae function as part of a highly mobile upper jaw. In *A. mento* these anterior processes consequently protrude in a ventral direction. This characteristic jaw protrusion shows by creating a beaklike appearance during prey capture, which is well-suited for picking (Alexander, 1967a). The premaxillae show an ascending as well as a descending arm (Fig. 4A, 5). The descending arms have a strongly ventrally recurved shape, whereby the impression of a beak gets further enhanced (Hernandez et al., 2018). A lip ligament connects the upper and lower jaws, and in case of movement, a broad tube-shaped mouth is formed, with the anterior tips of the upper and lower jaws placed in direct contact with the food item (Gibb et al, 2008).
The premaxillary and dentary teeth of *A. mento* (Fig. 4A/B, 6, 7A) are similar to other Old World and all New World cyprinodonts. The tricuspid outer teeth are also present in other cyprinodontiform fish of the genera *Jenynsia*, *Anableps*, *Oxyzygonectes* and *Cyprinodon variegatus* (Parenti, 1981; Hernandez et al., 2018).

The lower jaw has an **angulo-articular** and a **dentary bone** (Fig. 4A-C, 7A). Like in most teleosts, the angular in *A. mento* has a typically triangular form (Fig. 7B), with an anterior process that fits between the coronoid as well as the ventral processes of the dental (Fig. 7A). *A. mento* has a derived lower jaw, which is characterized by the posterior expansion of Meckel's cartilage (Parenti, 1981). Compared to other cyprinodontiforms (Parenti, 1981), it covers a large part of the articular (Fig. 8).

#### 5.4.2.2 Suspensorium

The **suspensorium** represents a sequence of cartilages and bones, including the **pterygoid** series (1, 4B, 7), the **palatine** (4A/B), and the **quadrate** (Fig. 4B, 6B, 9), a paired, triangular shaped, endochondral bone, that connects the lower jaw to the palatine and hyoid arch (Westneat, 2006).

#### 5.4.2.3 Hyoid apparatus

The **hyoid apparatus** is the primary element of the floor of the mouth that may move ventrally to enhance the expansion of the buccal cavity during suction feeding (Westneat, 2006).
It includes an **urohyal** (Fig. 12A-D), **basihyal**, **hypohyal** (Fig. 10A-D), **ceratohyal** (Fig. 10A-D), **epihyal** (Fig. 12A-D), **interhyal** and **branchiostegal rays** (Fig. 12A-D) (Aerts, 1991; Faustino and Power, 2001; Helfman et al., 2009; Huby and Parmentier, 2019).
Because the hyoid apparatus articulates via the median side of the hyomandibula with the suspensorium to the branchial basket, a back-and-forth movement of the buccal roof is possible (Liem, 1967; Osse, 1969).

#### 5.4.2.4 Opercular apparatus

The **opercular apparatus** (Fig. 13A-D) consists of four pairs of flat dermal bones. They form the gill covers and therefore protect the underlying gill arches. They are involved in respiration and feeding (Helfman et al., 2009).
The operculo-mandibular coupling is another pathway for exerting force on the mandible for jaw depression (Westneat, 2006). The opercle has an anterior articulation facet (Fig. 13C) connecting with the hyomandibula (Helfman et al., 2009).
In many species, the **sub-** and **interopercle** are free to move relative to the **preopercle** and can therefore be pulled posteriorly by the motion of the opercle (Westneat, 2006). Furthermore, Westneat (2006) postulates that in more derived teleosts a robust interoperculo-mandibular should be present. It attaches the interopercle (Fig. 13A/B) to the posteroventral margin of the lower jaw. So, if the interopercle is pulled posteriorly, this action gets transmitted to the lower jaw, leading to a depression of the lower jaw. Consequently, it can be expected that this ligament is present in *A. mento* too. However, the ligaments were hard to distinguish in the microCT scans, so its existence in *A. mento* is yet to be confirmed.

### 5.4.2.5 Pharyngeal jaw apparatus (PJA)

The **pharyngeal jaw apparatus (PJA)** in Cyprinodontidae is a well-developed system of muscles and bones that functions in different prey processing behaviors. Due to the specialization of prey processing, the PJA complements the prey manipulation of the oral jaw apparatusand separates food, what increases the overall diversity of feeding behavior seen in fish (Wainwright, 2005).

The PJA is formed from modified branchial arch elements and includes the gill arches, branchial muscles and ligaments, as well as the articular capsules which connect the gill arch elements (Lauder, 1983).

The pharyngeal jaws are bony elements that can show high variability in their structure (Fig. 14A-D). Numerous studies in Cichlidae (Greenwood, 1965; Ismail et al., 1982; Kornfield and Taylor, 1983; Hoogerhoud, 1984; Meyer, 1987, 1990a, b; Witte et al., 1990; Kornfield, 1991; Huysseune et al., 1994) and Salmonidae (Alexander & Adams, 2004) demonstrate that the skeletal elements are involved in important functional relations in trophic specialization (Ferrito et al., 2007). The lower pharyngeal jaw is actually the most posterior, and therefore in most cases the **fifth ceratobranchial** (Fig. 14A-D). The upper pharyngeal jaw persists of several merged **pharyngobranchials** (Fig. 14A-D). The PJA is used to crack hard-shelled prey items, to separate edible from inedible material, to chew, and to transport prey into the esophagus (Wainwright, 2005). Therefore, both jaws of the PJA bear teeth, that vary depending on the food type of the fish. They not only vary functionally among species showing different food types, but may also develop differently among individuals of a population as a function of the food types encountered by the growing fish (Helfman et al., 2009).

The surface of the pharyngeal jaws in species that primarily feed on hard prey and therefore always use the pharyngeal jaws in a crushing pattern, differ from the pharyngeal jaws of species that use the crushing behavior only when hard prey is consumed (Horn and Ferry-Graham, 2006). For example, the Cichlid fish of Cuatro Cienegas (Mexico), *Cichlasoma minckleyi*, show that individuals that feed on plants develop small pappiliform pharyngeal dentition, whereas those that feed on snails develop robust molariform dentition (Kornfield & Taylor 1983; Helfman et al., 2009).

The musculoskeletal couplings involved in gill arch movement extend beyond the branchial apparatus to connect to the mandible, hyoid, neurocranium and the pectoral girdle.

## 5.5 Cranial musculature

### 5.5.1 Ocular muscles

One important sensory system for most fish is vision. Some species even hunt primarily via the visual input they get. Therefore the eye muscles have been included in this thesis.

There are a lot of similarities between a fish eye and the eye of terrestrial vertebrates including humans (Helfman et al, 2009). However, one difference is that fish have a more spherical lens. While birds and mammals normally adjust focus by changing the shape of their lens, fish adjust focus by moving the lens closer to or further from the retina (Helfman et al, 2009).

Extrinsic eye muscles move the eye within its orbit (Helfman et al, 2009). These muscles are evolutionary very conservative, which means that vertebrates typically have the same three pairs of this striated muscles: **inferior** or ventral and **superior** or dorsal **oblique**; **inferior** or ventral and **superior** or dorsal **rectus**; and **external** or lateral and **internal** or medial **rectus** (Fig. 16A-C) (Helfman et al., 2009). These six extraocular muscles control the pursuit and saccade movements that are required to track prey and maintain stable images on the retina for high acuity vision (Kasprick et al., 2011).

### 5.5.2 Mandibular muscles

In general there are seven principal muscles involved in opening and closing the jaws, suspensorium and operculum during feeding and breathing (Helfman et al., 2009), with the **adductor mandibulae** (Fig. 17A/B, 18A-D) as one of the largest and most striking muscles of the cheek (Westneat, 2006).

The adductor mandibulae complex primarily serves the movement of the skeletal elements associated to the mandibular arch, and therefore powers the bite of the mandible by being responsible for closing the jaws (Westneat, 2006). Therefore, it is the main head and the most powerful feeding musculature (Werneburg, 2015). This muscular complex is highly adapted to different feeding strategies among vertebrate clades and therefore displays a large amount of diversification (Gosline, 1986; Diogo, 2008; Diogo & Abdala, 2010; Datovo & Vari, 2013; Werneburg 2015).

It is hypothesised that the adductor mandibulae became subdivided early on in the history of the neopterygians and almost certainly by the paleoniscid stage (Schaeffer and Rosen, 1961; Winterbottom, 1973).

The adductor mandibulae musculature is usually subdivided into two or more muscle subdivisions, leading to a complex of individual muscles that have a separated origin, course, and insertion (Werneburg, 2015). This is also the case in *A. mento* (Fig. 17A/B, 18A-D).
Here, the first division of the adductor mandibulae **(A1)** extends from the suspensorium and preopercle to an insertion on the ventral third of the maxilla (Fig. 17A) similar to *Belonesox belizanus, Fundulus rubrifrons* and *Gambusia affinis* (Ferry-Graham et al., 2010). Furthermore, the main adductor mandibulae A1 is divided in **A1α** and **A1β**, showing another similarity between *A. mento* and *Fundulus sp.* (Hernandez et al., 2008). While in many cyprinodontiforms the adductors mandibulae **A2** and **A3** form one largely united mass, in *A. mento* A2 and A3 are, similar to *Belonesox belizanus*, more distinct (Fig. 17B) (Ferry-Graham et al., 2010).

### 5.5.3 Hyoid muscles

The hyoid muscles play an important role in the mouth opening, as well as motions of the hyoid apparatus (Huby and Parmentier, 2019).
They include the **protractor hyoideus** (Fig. 22A/B), **hyohyoideus**, **adductor operculi** (Fig. 21A/B) and **adductor arcus palatini** (Fig. 19A-C, 20).

While the sternohyoideus (Fig. 22A/B), a hypobranchial muscle, pulls the hypobranchial system backward, the **protractor hyoideus** may pull this system forward (Vandewalle et al., 2000).
The protractor hyoideus connects the hyoid arch to the dentary. It is formed by the interhyoideus that fused with the intermandibularis posterior (Winterbottom, 1973). The anterior region of the protractor hyoideus is subdivided into a dorsal part, also known as geniohyoideus posterior, and a ventral part, also referred to as geniohyoideus anterior (Fig. 22A/B). In general there are a lot of controversies in regard of these muscles function and embryology (Winterbottom, 1973). While the ventral part of the protractor hyoideus is contracted during expiration, the dorsal part of the same muscle contracts mainly during inspiration (Winterbottom, 1973).

The **hyohyoideus** is a ventral muscle that is in contact with the hyoid apparatus. In higher actinopterygians it is subdivided into **hyohyoideus inferior** (Fig. 22A/B) and **superior** (Huby and Parmentier, 2019). The latter is further divided into **hyohyoideus abductor** and **adductors** (Fig. 22A/B).
While the hyohyoideus adductors are responsible for the constriction of the branchiostegal membrane, the abductors are responsible for its expansion.

The **adductor operculi** (Fig. 21A/B) is a dorsal positioned hyoid muscle that is present in all actinopterygians (Huby and Parmentier, 2019). It has attachment sites at the neurocranium and the opercles, causing their adduction.
Furthermore, the opercle gets operated by broad fleshy **dilatator** (Fig. 20, 21A/B) and **levator operculi** muscles (Fig. 18A/B). These muscles serve to expand the branchial chamber and draw in water. Therefore, they create a posterior displacement of the opercular series via contraction of the levator operculi and a lateral motion via contraction of the dilatator operculi (Gregory, 1933; Westneat, 2006).

Driven by **adductor** and **levator arcus palatini** muscles (Fig. 19A-C, 20), the hyomandibula as well as the suspensorium are often flared laterally during feeding (Westneat, 2006).
In lower teleosts the adductor arcus palatini connects the prootic to the dorso-medial face of the hyomandibular (Dietz, 1914, Edgeworth, 1935; Winterbottom, 1973). In *A. mento* this muscle originates from the ventrolateral margin of the parasphenoid. It has expanded anteriorly underlying the orbit (Fig. 19A-C, 20).
In *A. mento* both the levator arcus palatini and the dilatator operculi are superficial and sequential muscles lying between the rear of the orbit and the posterodorsal tip of the opercle (Winterbottom, 1973) (Fig. 20).

## 5.5.4 Branchial muscles

Within teleosts, four **external** (Fig. 21A/B, 25A/B) and two **internal levators** (Fig. 24A/B) are usually present (Winterbottom, 1973). In *A. mento* these two internal levators are running from the neurocranial base to the pharyngobranchial elements. Both the external and internal levator muscles lift, protract and abduct the **upper pharyngeal jaws** (UPJs) (Vandewalle et al., 1994). If the midpoints of the epibranchials are constrained, they can be rotated about this point by action of the **levator posterior** and second, third and fourth **levator externus**, that connect the lateral margins of the epibranchials to the neurocranium (Wainwright, 2005). So, the contraction of the external levators can cause lateral spreading of both upper pharyngobranchial jaw bones (Vandewalle et al., 1994).
However, if the joints between the pharyngobranchials and the epibranchials 2 to 4 are flexed, while the midpoint of the epibranchials are constrained or pulled ventrally by the **adductor branchialis** muscles 2 to 4 (Fig. 29A/B) and the **obliquus posterior** muscles (Fig. 29A/B), the epibranchial bones start to rotate ventrally. Therefore they, similar to perciforms, press on the

dorsal surface of the UPJs, depressing them (Wainwright, 2005). The joints between the epi- and pharyngobranchials can also be flexed by the **obliquus dorsalis muscle** directly.
Another important part of the dorsal region of the branchial arches is the **retractor dorsalis** muscle (Fig. 23A/B). It originates from the ventral side of the neurocranium and runs to the merged pharyngobranchials, as well as to the ventral side of the anterior vertebrae (Vandewalle et al., 1994). It retracts and inclines the UPJs caudally and therefore is an antagonist to the levator complex.
In the dorsal region of the branchial arch, there are mostly two **transversus dorsalis** muscles present. In *A. mento* they are located next to each other (Fig. 26A/B, 27), with the anterior transversus dorsalis muscle being bigger than the posterior transversus dorsalis muscle. These muscles, connect the dorsal elements of the branchial arches across the midline (Winterbottom, 1973).

Concerning the ventral parts of the gill arches, most fish possess at least **obliqui ventrales** 1-3 (Fig 28B/C), **rectus ventralis** 4 (Fig. 28A/B), **transversi ventrales** 4-5 (Fig 28A/B) (also known as transversus ventralis anterior and posterior) and a **rectus communis** (Fig. 22A) (Winterbottom, 1973).
The obliqui ventrales connect the ventral surfaces of the hypobranchial and ceratobranchial elements of the first three branchial arches (Fig. 28A/B).
In general it is debated whether the transversi ventrales (together with the paired recti ventrales) represent the plesiomorph condition for Teleostei and the obliqui ventrales developed from them (Edgeworth, 1935; Winterbottom, 1973), or whether it is the other way around (Kesteven, 1943; Nelson, 1967a; Winterbottom, 1973). However, because the embryonic branchial muscle plates do not meet in the ventral midline (Kesteven, 1943) and no "generalized" teleost is known to have an obliquus ventralis and transversus ventralis on the same arch (Nelson, 1967a), and furthermore, because the obliquus ventralis muscle always occurs when both hypo- and ceratobranchial elements are present, the latter hypothesis seems more likely (Kesteven, 1943; Nelson, 1967a; Winterbottom, 1973). Furthermore, this hypothesis seems to indicate that the transversus ventralis 4 developed with the loss of hypobranchial 4 (Winterbottom, 1973). The pharyngeal apparatus often also includes two transversi ventrales. They bridge a gap between the fourth and fifth pair of ceratobranchials (Fig. 28A/B). The simultaneous contraction of transversus ventralis 4 (Fig. 28A/B), uniting left and right ceratobranchials 4, and transversus ventralis 5 (Fig. 28A/B), uniting left and right ceratobranchials 5, probably allows these two bones to act as a single toothed element (Wainwright, 1989b; Bertucci et al., 2014). This is because

the lower pharyngeal jaws move towards each other when they contract (Vandewalle et al., 1994).

The number of recti ventrales in teleosts is variable. These muscles interconnect the hypobranchial, ceratobranchial or both elements of one arch to the preceding one (Winterbottom, 1973). In *A. mento,* there are three recti ventrales (r.vent 2, r.vent 3, r.vent 4) present (Fig. 28A/B).

According to Winterbottom (1973), in the more generalized neoteleosts the rectus communis muscle (Fig. 21A) connects the hypobranchial 3 to the ceratobranchial 5 (Winterbottom, 1973). However, the insertions can vary between species (Dietz 1912; Nelson 1969; Greenwood 1971; Winterbottom 1973; Vandewalle et al., 1994). In more advanced teleosts the anterior attachment site is shifted forward to the urohyal. This is also the case in *A. mento* (Fig. 22A). It is debated, if this muscle derived from the anterior growth of rectus ventralis 5 (Edgeworth, 1935; Millard, 1966), or if it developed from the back growth and splitting off of the ventral fibers of rectus ventralis 4 (Nelson 1976a; Winterbottom, 1973). Furthermore, Nelson (1976a, 1976b) suggested that, because this muscle, which depresses and therefore moves the lower pharyngeal jaws (LPJs) caudally, was present in anguilliforms and other teleosts, but not in *Elops*, it had arisen more than once during the evolution of teleosts (Winterbottom, 1973).

To date, only a limited number of studies have investigated the kinematics and muscle activity patterns of food processing by the pharyngeal apparatus. In many of these studies, biologists depend upon recording of voltage fluctuations due to action potentials within the muscle using electromyography (Westneat, 2006). Researchers are able to compile a motor activity pattern for suction feeding in a particular individual or species, by recording and measuring voltage patterns (electromyograms) of multiple muscles. Afterwards, these motor activity patterns are used with kinematics for assessing the functional role of muscles in driving feeding kinematics (Osse, 1969; Liem, 1978; Lauder, 1979; Westneat, 2006), comparing motor profiles between species, or testing for intraspecific differences between behaviors (Sanderson, 1988; Wainwright and Lauder, 1992; Grubich, 2001; Westneat, 2006). Since it is difficult to infer jaw kinematics solely from electromyography patterns or predict muscular activities from observed displacements, postulations must always be interpreted with caution (Lauder and Liem, 1983; Wainwright, 1989a; Claes and De Vree, 1992).

However, all specializations concerning the morphology of the branchial musculature, are obviously related to an increased participation of the pharyngeal jaws in the processing of food (Vandewalle et al., 1994).

### 5.5.5 Hypobranchial muscles

In basal actinopterygians such as Cladistia (e.g. *Polypterus senegalus*) two **hypobranchial muscles**, the **sternohyoideus** and the **coracomandibularis** are present (Noda et al., 2017). *A. mento* shows just a single hypobranchial muscle, the sternohyoideus (Fig. 22A). It plays a major role in hyoid depression.

A study of Lauder (1980a) has shown that the ventral hypaxial muscles stabilize the pectoral girdle and therefore provide an anchor point for the action of the sternohyoideus muscle. When the sternohyoideus contracts, the hyoid is pulled posteroventrally and this action is transferred directly to the mandible. Due to the retraction of the hyoid, the volume of the mouth for suction increases and causes the lower jaw rotation downwards (Aerts, 1991; Westneat, 2006).

## 5.6 Pectoral girdle musculature

Further posterior, behind the head of *A. mento,* muscles connecting the clavicula with the neurocranium as well as the pharyngeal jaws are present. One of them is the levator pectoralis (Fig. 30A/B), which seems to be a fairly late development during teleosts evolution, although its precise distribution among these fishes has yet to be determined (Winterbottom, 1973).

The musculature grouped in this region has only its attachment to the pectoral girdle in common. As Winterbottom (1973) describes, they derive from such a variety as the hypobranchial musculature (sternohyoideus and sternobranchialis), the fifth branchial arch muscle plate (pharyngoclavicularis and probably the protractor pectoralis) and the epaxial body musculature (levator pectoralis). The protractor pectoralis (Fig. 30A/B) connects the neurocranium and the pectoral girdle (Wainwright, 2005). It protracts the pectoral girdle, which probably acts to stabilize and protract the LPJ during prey crushing (Wainright, 2005). This mechanism is important for durophagous species feeding on hard-shelled organisms.

## 5.7 Breathing and feeding biomechanics

### 5.7.1 Breathing

The respiratory cycle of actinopterygians normally begins with mouth opening that implies the ventral rotation (i.e. depression) of the lower jaw (Huby and Parmentier, 2019). The lower jaw lowers because of individual or simultaneous contraction of sternohyoideus (Fig. 22A/B), the levator operculi (Fig. 21A/B), the epaxial and hypaxial muscles, and sometimes the geniohyoideus (i.e. protractor hyoideus) (Fig. 22A/B).

Immediately after jaw depression the hyoid apparatus rotates ventrally and the suspensorium expands laterally, due to the contraction of the sternoyoideus (Fig. 22A/B) and the levator arcus palatini (Fig. 19A-C, 20).

The expansion of the suspensorium may further be accomplished by the cooperation of the protractor hyomandibularis, also known as levator arcus palatini (Winterbottom, 1973), with the ventral muscles of the mandible, as well as a contraction of the adductor hyomandibularis (a synonym for adductor arcus palatini) (Fig. 19A-C, 20), intermandibularis (Fig. 22A/B) and adductor mandibulae (Edwards, 1926; Winterbottom, 1973). Due to the volume increase, the water is moved from the buccal to the pharyngeal cavity. If the opercular series is spread, the water flows towards the opened gills. The mouth closing, the rising of the hyoid apparatus and the adduction of the suspensorium increase the pressure and the water gets ejected from the opercular cavity.

Afterwards the opercular series returns to its prior position and the animal is ready to start a new respiratory cycle.

## 5.7.2 Jaw protrusion

Jaw protrusion is a major structural specialization in teleosteans that is related to the increasing mobility of the premaxilla and maxilla, which are loosely connected by ligaments (Huby and Parmentier, 2019).

The general mechanism of jaw protrusion has already been explained in the introduction, however there are a lot of different theories how such protrusion may be triggered.

*A. mento* shows, according to Motta (1984), the Type B or "twisting maxilla model" when it comes to jaw protrusion. The bowlike curved maxilla shows an internal hook (Fig. 5), that reaches into a socket positioned under the head of the premaxilla (Motta, 1984). As the lower jaw is depressed, the maxilla is pulled forward. Due to the attached adductor mandibulae (Fig. 17A/B, 18A-D) it is also partially restrained. Therefore, the maxilla twists on its own axes, driving the premaxilla anteriorly, with its internal head. A similar type of jaw arrangement can be seen in *Poecilia sphenops, Fundulus sp.* and *Mugil sp.* (Motta, 1984).

Due to this type of jaw protrusion, the fish's mouth region shows a beaklike appearance, well-suited for picking prey from the surface of the water or the ground (Alexander, 1967a). In addition they are also able to feed via the mechanism of suction feeding, where they "pick" their prey out of the water column. Furthermore, this fish species may have the possibility to winnow prey by extracting small prey from a larger collection of items (Horn and Ferry-Graham, 2006).

This beaklike appearance can also be seen in *Gambusia affinis* and *Kryptolebias marmoratus* (Ferry-Graham et al, 2008).

# 6 Conclusion

The structure of the skeletal elements in combination with the associated musculature in *A. mento* lead to the conclusion that this species belongs to a group of most highly evolved teleost fish.

Concerning the mechanism of suction feeding, more precisely the associated mechanism of jaw protrusion, it is reasonable to conclude that within this species the maxilla is pulled forward, as the lower jaw is depressed. This Type B mechanism of jaw protrusion, also known as "twisting maxilla model" (Motta, 1984), can also be seen in *Fundulus*, another genus within the cyprinodontiformes.

Furthermore *A. mento's* mouth region shows a beaklike appearance, similar to *Gambusia affinis*, *Kryptolebias marmoratus* (Ferry-Graham, 2008). This beaklike appearance is well-suited for the mechanism of suction feeding, as well as picking prey from the surface of the water or the ground (Alexander, 1967a)

Unfortunately, a more detailed analysis was sometimes impossible due to technical difficulties. Nevertheless, this study is the first detailed description of *A. mentos* morphology and therefore has brought new insights concerning the anatomy of its feeding apparatus. Furthermore, it helps to understand the adaptive radiation among *Aphanius*. However, it also shows that more research is needed to determine the relationship between *A. mentos* feeding apparatus and its feeding methods.

# 7 Acknowledgments

First of all, I would like to thank my supervisor Dr. Christian Beisser for giving me the opportunity to write this thesis and for all his help and encouragement along the way. I want to thank Dr. Thomas Schwaha for introducing me to Amira, helping me with any problem I had with regard to the reconstruction and for taking all the pictures, and Dr. Patrick Lemell for his advice and help. I also want to thank Dr Stephan Handschuh for his insights into the microCTs and for conducting the microCT scans in the first place. All of them were ready to help me whenever I had any difficulties or questions. Moreover, I would like to thank the Vienna Zoo for providing specimen of *Aphanius mento* for the microCT scans and for the method of clearing and staining.

# 8 References

**Adriaens D., Aerts P., Verraes W. (2001)** Ontogenetic shift in mouth opening mechanisms in a catfish (Clariidae, Siluriformes): A response to increasing functional demands. Journal of Morphology, Vol.247, pp.197–216.

**Aerts P. (1991)** Hyoid Morphology and Movements Relative to Abducting Forces During Feeding in *Astatotilapia elegans* (Teleostei: CichIidae). Journal of Morphology, Vol.208, pp.323-345.

**Al Akel A.S., SulimanE.M. (2011)** Biological control agent for mosquito larvae: Review on the killifish, *Aphanius dispar dispar* (Rppel, 1829). African Journal of Biotechnology, Vol.10(44), pp.8683-8688.

**Alexander G.D., Adams C.E. (2004)** Exposure to a common environment erodes inherited between-population trophic morphology differences in Arctic charr. Journal of Fish Biology, Vol.64, pp.253–257.

**Alexander R.M. (1967a)** The functions and the mechanisms of the protrusible upper jaw of some acanthopterygian fish. Journal of Zoology, Vol.151, pp.43-64.

**Alexander R.M. (1967b)** Mechanics of the jaws of some atheriniform fish. Journal of Zoology, Vol.151, pp.233-255.

**Alexander R.M. (1969)** Mechanics of the feeding action of a cyprinid fish. Journal of Zoology, Vol.159, pp.1–15.

**Bellwood D.R., Choat J.H. (1990)** A functional analysis of grazing in parrotfishes (family Scaridae): the ecological implications. Environonmental Biology of Fishes, Vol.28, pp.189–214.

**Bergert B.A., Wainwright P.C. (1997)** Morphology and kinematics of prey capture in the syngnathid fishes *Hippocampus erectus* and *Syngnathus floridae*. Marine Biology, Vol.127, pp.563–570.

**Bertucci F., Ruppé L., Van Wassenbergh S., Compère P., Parmentier Eric. (2014)** New insights into the role of the pharyngeal jaw apparatus in the sound-producing mechanism of *Haemulon flavolineatum* (Haemulidae). The Journal of Experimental Biology, Vol.217(Pt 21), pp.3862-9.

**Caillet G.M., Love M.S., Ebeling A.W. (1986)** Age and growth. In: Caillet G.M., Love M.S. & Ebeling A.W., (Eds.)Fishes: a Field and laboratory Manual on their structure, Identification and Natural History. pp. 154-157.

**Caiola N., Sostoa A. (2005)** Possible reasons for the decline of two native toothcarps in the Iberian Peninsula: evidence of competition with the introduced Eastern mosquitofish. Journal of Applied Ichthyology, Vol.21, pp.358-363.

**Camp A.L., Roberts T.J., Brainerd E.L. (2015)** Swimming muscles power suction feeding in largemouth bass. Proceedings of the National Academy of Sciences, Vol.112(28), pp.8690.

**Carroll A.M., Wainwright P.C., Huskey S.H., Collar D.C., Turingan R.G. (2004)** Morphology predicts suction feeding performance in centrarchid fishes. The Journal of Experimental Biology, Vol.207, pp.3873–3881.

**Carvalho M., Vari R.P. (2015)** Development of the splanchnocranium in Prochilodus argenteus (Teleostei: Characiformes) with a discussion of the basal developmental patterns in the Otophysi. Zoology, Vol.118(1), pp.34–50.

**Claes G., De Vree F. (1992)** Pharyngeal muscle activities during food processing in Oreochromis niloticus (Pisces: Cichlidae). Zoologisches Jahrbuch der Anatomie, Vol.122, pp.173-178.

**Datovo A., Vari R.P. (2013)** The jaw adductor muscle complex in teleostean fishes: Evolution, homologies and revised nomenclature (Osteichthyes: Actinopterygii). PLoS ONE 8(4):e60846

**Dietz P.A. (1912)** Vergelijkende anatomie van de kaaken kieuwboogspieren der Teleostei. PhD Thesis, University of Leiden

**Dietz P.A. (1914)** Beiträge zur Kenntnis der Kiefer- und Kiemenbogenmuskulatur der Teleostier. I. Die Kiefer- und Kiemenbogenmuskeln der Acanthopterygii. - Mitteilungen Statzione zoologica Neapel, Vol.22(4), pp.99-162.

**Diogo R. (2008)** The origin of higher clades: osteology, myology, phylogeny and evolution of bony fishes and the rise of tetrapods. Enfield: Science Publishers.

**Diogo R., Abdala V. (2010)** Muscles of vertebrates: comparative anatomy, evolution, homologies and development. Enfield: Science Publishers.

**Eaton T.H. (1935)** Evolution of the upper jaw mechanism in teleost fishes. Journal of Morphology, Vol.58(1), pp.157-172.

**Echelle A.A., Dowling T.E., (1992)** Mitochondrial DNA variation and evolution of the Death Valley pupfishes (*Cyprinodon*, Cyprinodontidae). Evolution, Vol.46, pp.193–206.

**Edgeworth F.H. (1935)** The Cranial Muscles of the Vertebrates. - Cambridge University Press. Vol.493, pp.841.

**Edwards L.F. (1926)** The protractile apparatus of the mouth of catostomid fishes. Anatomical Record, Vol.33(4), pp.257-270.

**El Safi S.H., Haridi A.A., El Rabaa F.M. (1985)** The impact of the exotic fish *Gambusia affinis* (Baird and Girard) on some natural predators of immature mosquitoes. The Journal of Tropical Medicine and Hygiene, Vol.88, pp.175-178.

**Engeman J.M., Aspinwall N., Mabee P.M. (2009)** Development of the pharyngeal arch skeleton in Catostomus commersonii (Teleostei: Cypriniformes). Journal of Morphology, Vol.270, pp.291–305.

**Faustino M., Power D.M. (2001)** Osteologic development of the viscerocranial skeleton in sea bream: alternative ossification strategies in teleost fish. Journal of Fish Biology, Vol.58(2), pp.537–572.

**Ferrito V., Mannino M.C., Pappalardo A.M., Tigano C. (2007)** Morphological variation among popultions of *Aphanius fasciatus* Nardo, 1827 (Teleostei, Cyprinodontidae) from the Mediterranean. Journal of Fish Biology, Vol.70(1), pp.1-20.

**Ferry-Graham L.A., Gibb A.C., Hernandez L. P. (2008)** Premaxillary movements in cyprinodontiform fishes: An unusual protrusion mechanism facilitates ‘‘picking’’ prey capture. Zoology, Vol.111(6), pp.455-466.

**Ferry-Graham L.A, Lauder G.V. (2001)** Aquatic prey capture in ray-finned fishes: a century of progress and new directions. Journal of Morphology, Vol.248, pp.99-119.

**Ferry-Graham L.A., Hernandez L.P., Gibb A.C., Pace C. (2010)** Unusual kinematics and jaw morphology associated with piscivory in the poecilid, *Belonesox belizanus*. Zoology, Vol.113(3), pp.140-147.

**Gibb A.C., Ferry-Graham L.A. (2005)** Cranial movements during suction feeding in teleost fishes: Are they modified to enhance suction production? Zoology, Vol.108(2), pp.141-153.

**Gibb A., Ferry-Graham L., Hernandez L., Romansco R., Blanton J. (2008)** Functional significance of intramandibular bending in Poeciliid fishes. Environmental Biology of Fishes, Vol.83(4), pp.507-519.

**Gillis G.B., Lauder G.V. (1995)** Kinematics of feeding in bluegill sunfish: is there a general distinction between aquatic capture and transport behaviors? The Journal of Experimental Biology, Vol.198, pp.709–720.

**Goodrich J.S., Sanderson S.L., Batjakas I.E., Kaufman L.S. (2000)** Branchial arches of suspension-feeding *Oreochromis esculentus*: sieve or sticky filter? Journal of Fish Biology, Vol.56, pp.858–875.

**Gosline W.A. (1986)** Jaw muscle configuration in some higher teleostean fishes. Copeia, Vol.3, pp.705–713.

**Greenwood P.H. (1965)** Environmental effects of the pharyngeal mill of a cichlid fish, *Astatoreochromis alluaudi* and their taxonomic implications. Proceedings of the Linnean Society of London Vol.176, pp.1–10.

**Greenwood P.H., Rosen D.E., Weitzman S.H., Myers G.S. (1966)** Phyletic studies of teleostean fishes, with a provisional classification of living forms. Bulletin of the American Museum of Natural History Zoology, Vol.131, pp.341-444.

**Greenwood P.H. (1971)** Hyoid and ventral gill arch musculature in osteoglossomorph fishes. Bulletin of the British Museum (Natural History) Zoology, Vol.22, pp.1-55.

**Gregory W.K. (1933)** Fish skulls: A study of the evolution of natural mechanisms. American Philosophical Society, Vol.23(2), pp.75-481.

**Grubich J. R. (2001)** Prey capture in actinopterygian fishes: A review of suction feeding motor patterns with new evidence from an elopomorph fish, *Megalops atlanticus*. American Zoologist, Vol.41, pp.1258–1265.

**Güçlü S.S., Küçük F. (2008)** Population Age, Sex Structure, Growth and Diet of *Aphanius mento* Heckel in: Russegger, 1843 (Cyprinodontidae: Teleostei), at Kırkgöz Spring, Antalya-Türkiye. Turkish Journal of Fisheries and Aquatic Sciences, Vol.8, pp.269-274.

**Güçlü S.S. (2012)** Population structure of Killifish, *Aphanius anatoliae* (Cyprinodontidae) endemic to Anatolia in Lake Eğirdir-Isparta (Turkey). Iranian Journal of Fisheries Sciences, Vol.11(4), pp.786-795.

**Handschuh S., Beisser C.J., Ruthensteiner B., Metscher B.D. (2017)** Microscopic dual-energy CT (microDECT): a flexible tool for multichannel ex vivo 3D imaging of biological specimens. Journal of Microscopy, Vol.267(1), pp.3-26.

**Haq S., Srivastava H.C. (2013)** Efficacy of *Aphanius dispar* (Rüppell) an indigenous larvivorous fish for vector control in domestic tanks under the Sardar Sarovar Narmada project command area in District Kheda, Gujarat. Journal of vector borne diseases, Vol.50(2), pp.137-40.

**Helfman G.S., Clark J.B. (1986)** Rotational feeding: overcoming gapelimited foraging in anguillid eels. Copeia 1986, pp.679–685.

**Helfman G., Collette B.B., Facey D.E., Bowen B.W. (2009)** The diversity of fishes: biology, evolution, and ecology. Oxford [u.a.] : Wiley-Blackwell. pp.30-31, pp.41-43, pp.157.

**Hernandez L.P., Ferry-Graham L.A., Gibb A.C. (2008)** Morphology of a picky eater: A novel mechanism underlies premaxillary protrusion and retraction within cyprinodontiforms. Zoology, Vol.111(6), pp.442-454.

**Hernandez L.P., Adriaens D., Martin C.H., Wainwright P.C., Masschaele B., Dierick M. (2018)** Building trophic specializations that result in substantial niche partitioning within a young adaptive radiation. Journal of Anatomy, Vol.232(2), pp.173-185.

**Hoogerhourd J.C. (1984)** A taxonomic reconsideration of the haplochrom in genera *Gaurochromis* GREENWOODD 1980 and *Labrochromis* Regan 1920 (Pisces, Cichlidae). Netherlands Journal of Zoology, Vol.34, pp.539-565.

**Horn M.H., Ferry-Graham L.A. (2006)** Feeding Mechanisms and Trophic Interactions. The Ecology of Marine Fishes, Chapter 14, University of California Press

**Hrbek T., Meyer, A. (2003)** Closing of the Tethys Sea and the Phylogeny of Eurasian Killifishes (Cyprinodontiformes: Cyprinodontidae). Journal of Evolutionary Biology, Vol.16, pp.17-36.

**Huby A., Parmentier E. (2019)** Actinopterygians: Head, Jaws and Muscles. In: Ziermann, J.M., Diaz R.E.Jr., Diogo R. (Eds.), Heads, Jaws, and Muscles : Anatomical, Functional, and Developmental Diversity in Chordate Evolution. Springer, pp. 93-142.

**Huysseune A., Sire J.Y., Meunier F.J. (1994)** Comparative study of lower pharyngeal jaw structure in two phenotypes of *Astatoreochromis alluaudi* (Teleostei: Cichlidae). Journal of Morphology, Vol.221, pp.25–43.

**Ismail M.H., Verraes W., Huysseune A. (1982)** Developmental aspects of the pharyngeal jaws in *Astatotilapia elegans* (Trewavas, 1933) (Teleostei: Cichlidae). Netherlands Journal of Zoology, Vol.32, pp.513–543.

**Kardong K.V. (2012)** Vertebrates: Comparative Anatomy, Function, Evolution 6th ed. New York: McCraw-Hill.

**Kasprick D., Kish P., Junttila T., Ward L., Bohnsack B., Kahana A. (2011)** Microanatomy of Adult Zebrafish Extraocular Muscles. PLoS One, Vol.6(11), E27095.

**Kesteven H.L. (1943)** The evolution of the skull and cephalic muscles. I. The fishes. -Memoirs of the Australian Museum, Vol.8(2), pp.65-132.

**Kornfield I. (1991)** Genetics. In: Keenleysid M.H.A. (Eds.): Cichlid Fishes, Behaviour, Ecology and Evolution, pp.103-128.

**Kornfield I., Taylor J.N. (1983)** A new species of polymorphic fish, *Cichlasoma minckleyi* from Cuatro Cienegas, Mexico (Teleostei: Cichlidae). Proceedings of the Biological Society of Washington, Vol.96, pp.253–269.

**Lauder G. V. (1979)** Feeding mechanisms in primitive teleosts and in the halecomorph fish Amia calva. Journal of Zoology (Lond.) Vol.187, pp.543–578.

**Lauder G.V. (1980a)** Evolution of the feeding mechanism in primitive actinopterygian fishes: a functional anatomical analysis of *Polypterus*, *Lepisosteus*, and *Amia*. Journal of Morphology, Vol.163, pp.283–317.

**Lauder G.V. (1980b)** Hydrodynamics of prey capture by teleost fishes. D. Schenk, ed. Biofluid Mechanics. Plenum, New York, Vol.2, pp. 161–181.

**Lauder G.V. (1980c)** The suction feeding mechanism in sunfishes (*Lepomis*): an experimental analysis. The Journal of Experimental Biology, Vol.88, pp.49–72.

**Lauder G.V.** (1982) Patterns of evolution in the feeding mechanism of actinopterygian fishes. American Zoologist. Vol.22, pp.275-285.

**Lauder G.V. (1985)** Aquatic feeding in lower vertebrates. In: Hildebrand, M., Bramble, D.M., Liem, K.F., Wake, D.B. (Eds.), Functional Vertebrate Morphology. Harvard University Press, Cambridge, MA, pp. 210–229.

**Lauder G.V., Liem K.F. (1981)** Prey capture by *Luciocephalus pulcher*: implications for models of jaw protrusion in teleost fishes. Environmental Biology Fish, Vol.6, pp.257–268.

**Lauder G.V., Liem K.F. (1983)** Functional design and evolution of the pharyngeal jaw apparature in euteleostean fishes. Zoological Journal of the Linnean Society, Vol.77, pp.1-38.

**Lauder G.V., Prendergast T. (1992)** Kinematics of aquatic prey capture in the snapping turtle, *Chelydra serpentina*. The Journal of Experimental Biology, Vol.164, pp.55–78.

**Lauder G.V., Reilly, S.M. (1994)** Amphibian feeding behavior: comparative biomechanics and evolution. In: Bels, V.L., Chardon, M., Vandewalle, P. (Eds.), Advances in Comparative and Environmental Physiology. Springer, New York, pp. 163–195.

**Lauder G.V., H.B. Shaffer (1985)** Functional morphology of the feeding mechanism in aquatic ambystomatid salamanders. Journal of Morphology, Vol.185, pp.297–326.

**Liem K. F. (1967)** Functional morphology of the head of the anabantoid Teleost fish *Helostma temmincki*. Journal of Morphology, Vol.121, pp.135-158.

**Liem K.F. (1973)** Evolutionary strategies and morphological innovations: cichlid pharyngeal jaws. Systematic Zoology, Vol.22, pp.425–441.

**Liem K F. (1978)** Modulatory multiplicity in the functional repertoire of the feeding mechanism in cichlid fishes. 1. Piscivores. Journal of Morphology, Vol.158, pp.323–360.

**Liem K.F., (1979)** Modulatory multiplicity in the feeding mechanism in cichlid fishes, as exemplified by the inverte- brate pickers of Lake Tanganyika. Journal of the Zoological Society of London, Vol.189, pp.93–125.

**Liem K.F. (1980a)** Adaptive significance of intra and interspecific differences in the feeding repertoires of cichlid fishes. American Zoolgist, Vol.20, pp.295-314.

**Meyer A. (1987**) Phenotypic plasticity and heterochrony in *Cichlasoma managuense* (Pisces, Cichlidae) and their implications for speciation in cichlid fishes. Evolution, Vol.41, pp.1357-1369.

**Meyer A. (1990a)** Ecological and evolutionary consequences of the trophic polymorphism in *Cichlasoma citrinellum* (Pisces: Cichlidae). Biological Journal of the Linnean Society, Vol.39, pp.279–299.

**Meyer A. (1990b)** Morphometrics and allometry in the trophically polymorphic cichlid fish, *Cichlasoma citrinellum*: alternative adaptations and ontogenetic changes in shape. Journal of Zoology, London Vol.221, pp.237–260.

**Michel K.B., Adriaens D., Aerts P., Dierick M., Wassenbergh S. Van (2014)** Functional anatomy and kinematics of the oral jaw system during terrestrial feeding *Periophthalmus barbarus*. Journal of Morphology, Vol.275(10), pp.NA-NA.

**Millard N.A.H. (1966)** Contributions to the functional morphology of fishes. Pt. I. Introduction. - Zoologica Africana, Vol.2,pp.37-43.

**Mordenti O., Di Biase A., Zaccaroni A., Bastone G., Scaravelli D. (2012)** Induced Reproduction of *Aphanius fasciatus* by Ecophysiological Conditioning and Hormonal Treatment in Fresh and Marine Water. The Israeli Journal of Aquaculture - Bamidgeh, Vol.64, pp.6.

**Moss S.A. (1977)** Feeding mechanisms in sharks. American Zoologist, Vol.17, pp.355–364.

**Motta P.J. (1984)** Mechanics and functions of jaw protrusion in teleost fishes: a review Copeia, No.1, pp:1-18.

**Muller M. (1987)** Optimization principles applied to the mechanism of neurocranium levitation and mouth bottom depression in bony fishes (Halecostomi). Journal of Theoretical Biology, Vol.126, pp.343–368.

**Muller M., Osse J.W.M. (1984)** Hydrodynamics of suction feeding in fish. Transactions of the Zoological Society of London, Vol.37, pp.51–135.

**Nelson G.J. (1967a)** Gill arches of some teleostean fishes of the families Girellidae, Pomacentridae, Embiotocidae Labridae and Scaridae. Journal of Natural History, Vol.1(2), pp.289-293.

**Nelson G.J. (1967b)** Branchial muscles in representatives of five eel families. Pacific Science, Vol. 21(3), pp.348-363.

**Nelson G.J. (1969)** Gill arches and the phylogeny of fishes, with notes on the classification of vertebrates. Bulletin of the American Museum of Natural History, Vol.141, pp.475-552.

**Noda M, Miyake T, Okabe M (2017)** Development of cranial muscles in the actinopterygian fish *Senegal bichir*, *Polypterus senegalus* Cuvier, 1829. Journal of Morphology, Vol.278(4), pp.450–463

**Norton S.F., Brainerd E.L. (1993)** Convergence in the feeding mechanics of ecomorphologically similar species in the Centrarchidae and Cichlidae. The Journal of Experimental Biology, Vol.176, pp.11–29.

**Osse, J.W.M. (1969)** Functional morphology of the head of the perch (*Perca fluviatilis*): an electromyographic study. Netherlands Journal of Zoology, Vol.19, pp.289–392.

**Parenti L.R. (1981)** A phylogenetic and biogeographic analysis of cyprinodontiform fishes (Teleostei Atherinomorpha).Bulletin of the American Museum of Natural History, Vol.168(4), pp.341-557.

**Parker A., Kornfield I. (1995)** Molecular perspective on evolution and zoogeography of cyprinodontid killifishes (Teleostei; Atherinomorpha). Copeia, pp.8–21.

**Parmentier E, Lo-Yat A., Vandewalle P. (1998)** Morphology of the buccal apparatus and related structures in four species of Carapidae. Australian Journal of Zoology, Vol.46(4), pp.391–404.

**Reichenbacher B., Kamrani E., Esmaeili H.R., Teimori A. (2009)** The endangered cyprinodont *Aphanius ginaonis* (Holly, 1929) from southern Iran is a valid species: evidence from otolithmorphology. Environmental Biology of Fishes, Vol.86(4), pp.507-521.

**Sanford C.P.J., Wainwright P.C. (2002)** Use of sonomicrometry demonstrates the link between prey capture kinematics and suction pressure in largemouth bass. The Journal of Experimental Biology, Vol.205, pp.3445–3457.

**Schaeffer B., Rosen D.E. (1961)** Major adaptive levels in the evolution of the actinopterygian feeding mechanism. American Zoologist, Vol.1, pp.187-204.

**Schaefer S.A., Lauder G.V. (1986)** Historical transformation of functional design: evolutionary morphology of feeding mechanisms in loricarioid catfishes. Systematic Zoology, Vol.35, pp.489–508.

**Schulz-Mirbach T., Reichenbacher B., Yildrim M.Z., Atalay M.A (2006)** Otolith characteristics of species, subspecies, and populations of *Aphanius* Nardo, 1827 (Teleostei, Cyprinodontiformes) from Anatolia (Turkey). Journal of Natural History, Vol.40(27-28), pp.1687-1705.

**Smith K.K. (1993)** The form of the feeding apparatus in terrestrial vertebrates: Studies of adaptation and constraint. In: Hanken J., Hall B.K. (Eds.). The Skull Vol. 3, Functional and Evolutionary Mechanisms. Chicago: University of Chicago Press, pp 150-196.

**Svaänback R., Wainwright P.C., Ferry-Graham L.A. (2002)** Linking cranial kinematics, buccal pressure, and suction feeding performance in largemouth bass. Physiological and Biochemical Zoology, Vol.75, pp.532–543.

**Teimori A., Esmaeili H.R., Erpenbeck D., Reichenbacher B. (2014)** A new and unique species of the genus *Aphanius* Nardo, (1827 (Teleostei: Cyprinodontidae) from Southern Iran: A case of regressive evolution. Zoologischer Anzeiger - A Journal of Comparative Zoology, Vol.253(4), pp.327-337

**van Damme J., Aerts P. (1997)** Kinematics and functional morphology of aquatic feeding in Australian snakenecked turtles (*Pleurodira*; *Chelodina*). Journal of Morphology, Vol.233(2), pp.113-123.

**Vandewalle P. (1972)** Ostéologie et myologie de *Tilapia guineensis* (Bleeker, 1862). Annales du Musée royal de l'Afrique Centrale, Sciences zoologiques, Vol.196, pp.50.

**Vandewalle P., Huyssene A., Aerts P., Verraes W. (1994)** The pharyngeal apparatus in Teleost feeding. In: Bels V.L., Chardon M., Vandewalle P. (Eds.) Biomechanics of Feeding in Vertebrates. Advances in Comparative and Environmental Physiology, Vol.18. Springer, Berlin, Heidelberg

**Vandewalle P., Saintin P., Chardon M. (1995)** Structures and movenments of the buccal and pharyngeal jaws in relation to feeding in *Diplodus sargus*. Université de Liège, Institut de Zoologie, Laboratoire de Morphologie fonctionnelle, 22 quai Van Beneden, B-4020 Liège, Belgium

**Vandewalle P., Parmentier E., Chardon M. (2000)** The Branchial Basket in Teleost Feeding. Cybium, Vol.24(4), pp.319-342.

**van Leeuwen J.L., Muller M. (1984)** Optimum sucking techniques for predatory fish. Transactions of the Zoological Society of London, Vol.37, pp.137–169.

**Wainwright P.C. (1989a)** Prey processing in Haemulid fishes: patterns of variation in pharyngeal jaw muscle activity. The Journal of Experimental Biology, Vol.141, pp.359-375.

**Wainwright, P. C. (1989b)** Functional morphology of the pharyngeal jaw apparatus in perciform fishes: an experimental analysis of the Haemulidae. Journal of Morphology, Vol.200, pp.231- 245.

**Wainwright P.C. (2005)** Functional Morphology of the Pharyngeal Jaw Apparatus. In: Shadwick R.E., Lauder G.V. (Eds.), Fish PhysiologyBiomechanics, Vol.23. San Diego, CA: Academic Press), pp.77-101.

**Wainwright P.C., Ferry-Graham L.A., Carroll A.M., Hulsey C.D., Waltzek T.B., Grubich J.R. (2001)** Evaluating the use of ram and suction during prey capture in cichlid fishes. The Journal of Experimental Biology, Vol.204, pp.3039–3051.

**Wainwright P.C., Day S.W. (2007)** The forces exerted by aquatic suction feeders on their prey. Journal of The Royal Society Interface, Vol.4, pp.553–560.

**Webb C., Joss J. (1997)** Does predation by the fish *Gambusia holbrooki* (Atheriniformes: Poeciliidae) contribute to declining frog populations? Austr. Zool., Vol.30, pp.316-324.

**Werneburg I. (2015)** Morphology of the jaw, suspensorial, and opercle musculature of Beloniformes and related species (Teleostei: Acanthopterygii), with a special reference to the m. adductor mandibulae complex. PeerJ, Vol.2015(2)

**Westneat M.W. (2006)** Skull Biomechanics and Suction Feeding in Fishes. In: Shadwick R.E., Lauder G.V. (Eds.), Fish Biomechanics. San Diego, CA: Academic Press), pp 29-75.

**Wildekamp R.H. (1993)** A World of Killies, Atlas of the Oviparous Cyprinodontiform Fishes of the World, The Genera *Adamas, Adinia, Aphanius, Aphyoplatys* and *Aphyosemion,* American Killifish Association, Inc., U.S.A.

**Wildekamp R.H., Küçük F., Ünlüsayın M. and Van Neer W. (1999)** Species and Subspecies of the Genus *Aphanius* Nardo 1897 (Pisces: Cyprinodontidae) in Turkey, Turkish Journal of Zoology, Vol.23, pp.23-44.

**Wilga C.D., Wainwright P.C., Motta P. J. (2000)** Evolution of jaw depression mechanics in aquatic vertebrates: Insights from Chondrichthyes. Biological Jornal of the Linnean Society, Vol.71, pp.165–185.

**Winterbottom R. (1973)** A Descriptive Synonymy of the Striated Muscles of the Teleostei. Proceedings of the Academy of Natural Sciences of Philadelphia, Vol.125, pp.225-317.

**Witte F., Barel C.D.N., Hoogerhoud R.J.C. (1990)** Phenotypic plasticity of anatomical structures and its ecomorphological significance. Netherlands Journal of Zoology, Vol.40, pp.278-298.